AN INVESTIGATION OF PRESSURE-DROP COEFFICIENTS FOR ORIFICE PLATES AND HONEYCOMB GRIDS

A THESIS

Presented to

the Faculty of the Graduate Division

by

David Bernstein

In Partial Fulfillment

of the Requirements for the Degree

Master of Science in Aeronautical Engineering

Georgia Institute of Technology

May 1953

In presenting the dissertation as a partial fulfillment of the requirements for an advanced degree from the Georgia Institute of Technology, I agree that the Library of the Institution shall make it available for inspection and circulation in accordance with its regulations governing materials of this type. I agree that permission to copy from, or to publish from, this dissertation may be granted by the professor under whose direction it was written, or, in his absence, by the Dean of the Graduate Division when such copying or publication is solely for scholarly purposes and does not involve potential financial gain. It is understood that any copying from, or publication of, this dissertation which involves potential financial gain will not be allowed without written permission.

_____

_____

AN INVESTIGATION OF PRESSURE-DROP COEFFICIENTS FOR ORIFICE PLATES AND HONEYCOMB GRIDS

Approved: _____

_____

_____

_____

_____

Date Approved by Chairman: June 3, 1955

ACKNOWLEDGEMENTS

The author wishes to express his appreciation to Professor J. J. Harper for his most generous aid, valuable criticisms, and complete guidance throughout the preparation of this thesis. Gratitude is extended to Professor A. L. Ducoffe and Professor C. E. Kindsvater for their review of the topic.

LIST OF SYMBOLS

A- area.

C- contraction ratio of a streamtube.

D- diameter of holes in an orifice plate; distance between centers of elements in a honeycomb grid.

L- length of elements of a honeycomb grid.

L/D- fineness ratio.

M- ratio of open area to total area.

P- static pressure.

P_{sc}- static pressure in settling chamber.

ΔP- difference in total pressure in front of and in back of a specimen.

$\Delta P/q$- pressure-drop coefficient.

q- dynamic pressure upstream of test section; $\rho V^2/2$.

R- Reynolds Number; $(\rho V/\mu)$x(a characteristic length).

S- solidity; ratio of solid area to total area; (1-M).

T- thickness of plate.

V- velocity.

W- width of solid material between edges of holes in an orifice plate; thickness of elements in a honeycomb grid.

α- angle of inclination of the airstream.

λ- angle between normal to the flow and an orifice plate; $(90^\circ - \alpha)$.

ρ- density of air.

μ- coefficient of dynamic viscosity of air.

TABLE OF CONTENTS

LIST OF TABLES

LIST OF FIGURES

LIST OF FIGURES (CONTINUED)

Figure Page

SUMMARY

An investigation was made of the pressure-drop coefficients of orifice plates and honeycomb grids of the type often used in wind tunnel research and design. The parameters investigated for the orifice plates were solidity, Reynolds Number, hole diameter with constant solidity, and angle of inclination to the flow. The parameters investigated for the honeycomb grids were solidity, Reynolds Number, and the ratio of the length of the grid to the spacing of the elements of the grid--that is, fineness ratio.

It was determined that for a given solidity and Reynolds Number of an orifice plate, the pressure-drop coefficient is a function of the hole size and the hole spacing. For orifice plates, the ratio of the square of the hole diameter to the width of the solid portion between the edges of the holes was chosen as the characteristic length in the evaluation of the Reynolds Number. The experimental points for pressure-drop coefficient versus solidity of an orifice plate agree favorably with the empirical equation developed with provision made for the variation of the contraction ratio at the vena contracta of a streamtube.

The investigation showed that the pressure-drop coefficient for an orifice plate of constant solidity will vary

as the square of the sine of the angle of inclination to the airstream except at angles less than 30 degrees.

The pressure-drop coefficient for honeycomb grids decreased rapidly with increasing Reynolds Number and then approached a constant value. The pressure-drop coefficient for a honeycomb grid of constant solidity and at constant Reynolds Number increased linearly with increasing length of the grid for $L/D > 2$.

CHAPTER I

INTRODUCTION

Orifice plates are often used in wind tunnel tests to simulate objects such as radiators and engines on wind tunnel models so that a given pressure drop can be obtained; an orifice plate is used rather than a scale model since a model will tend to distort the pressure drop because of the scale effect. Dive flaps, spoilers, and other devices intended to produce high drag on airplanes are often fabricated of flat metal plates through which holes are punched. These metal plates along with protective devices on jet engine inlets are much the same as orifice plates. While honeycomb grids are frequently used to straighten and smooth the airstream in windtunnels, there is little data pertaining to the pressure drop across honeycomb grids.

This investigation was made to extend and correlate with theory the existing data for pressure-drop coefficients of orifice plates, and to provide additional data for the design of honeycomb grids for use in wind tunnels.

Czarnecki (1) and Hoerner (2) conducted investigations of the pressure-drop characteristic of orifice plates in order to facilitate wind-tunnel tests and the design of high drag and protective devices; however, assumptions were made

in these investigations such that the results are inaccurate in the general case. Czarnecki (1) varied the solidity of the orifice plates by inserting corks in the holes of the plates and thereby obtained different pressure drops for different values of solidity at a given velocity. However, one should expect that for a given solidity, which is the ratio of solid area to total area of an orifice plate, it should be possible to obtain different pressure drops for a constant velocity and solidity. That is, the pressure drop across a plate of given solidity constructed of small holes which are close together will be less than that of another plate of the same solidity but having large holes spaced far apart. This is apparent from a consideration of the fact that in the former case the airstream passes through the orifice plate without encountering as many obstructions as in the latter case.

If different pressure-drop coefficients can be obtained for a given solidity by changing the geometry of the orifice plate, it is necessary to know the particular parameter of the geometry of the plate which will uniquely define the pressure-drop coefficient for a given solidity. The Reynolds Number should then have this parameter incorporated in it so that the pressure-drop coefficient will be uniquely defined for a given Reynolds Number and solidity.

Hoerner (2) developed a theoretical relationship

between the pressure-drop coefficient and the solidity; this relationship is based on the effective solidity and is independent of the Reynolds Number. The effective solidity is the geometric solidity corrected for the vena contracta of the streamtubes. Since the streamtubes contract after passing through the holes in an orifice plate, the solidity is increased as there is less resultant free space through which the airstream can pass. Hoerner (2) assumed that the contraction coefficient of the streamtubes is independent of the solidity and is a constant for a given edge condition of the holes in the orifice plate.

O'Brien (3) and Taylor (4) state that the contraction coefficient increases with increasing hole diameter and hence in general increases with decreasing solidity. Thus it is necessary to obtain a theoretical relationship between the pressure-drop coefficient and the geometric solidity taking into account the variation of the contraction of the streamtube with variation of solidity, hole size, and edge condition of the hole.

Since devices similar to orifice plates must frequently be used in such a manner that the device is at an angle of incidence to the airstream, the effect of varying the angle of incidence of an orifice plate is of interest. It can be shown that for an orifice plate which is placed obliquely in an airstream, the pressure-drop coefficient will vary as the square of the sine of the angle of incidence to

the airstream. Hoerner (2) states that such a variation is not strictly valid since the walls of the duct prevent the flow from developing fully, and that the variation of the pressure-drop coefficient with angle of incidence is approximately as the sine of the angle.

However, Schubauer (5), after tests of wire screens placed at angles of incidence to an airstream, came to the conclusion that the sine-squared law will hold true for wire screens. It appears that the sine-squared law should also be valid in the case of orifice plates if the pressure downstream of the orifice plate is measured far enough downstream so that there are no interference effects in the airstream. Hence an investigation of the effect of angle of incidence was made.

In the design of a windtunnel it is necessary to know the pressure drop across the honeycomb as a function of the length of the honeycomb for a given mesh or solidity. Since the length of a honeycomb grid is usually greater than the width of the elements, and the flow pattern immediately downstream of the grid is different from that of a wire screen, one should not expect that the relationships developed for wire screens to hold true for a honeycomb grid.

The effect of length is to produce an additional pressure drop due to the frictional losses along the length of the grid and expansion losses within the elements of the

grid. For small lengths, the frictional losses are negligible in comparison with the expansion losses; however, as the length of the grids increases, the frictional losses increase and are no longer negligible.

CHAPTER II

INSTRUMENTATION AND EQUIPMENT

The experimental work was performed in the Laboratory of the Daniel Guggenheim School of Aeronautics at the Georgia Institute of Technology.

The airstream was supplied by a Buffalo Forge Blower, number 5E, manufactured by the Buffalo Forge Company, Buffalo, N. Y., and powered by a 5 H.P. Sterling "Cros-Line" Motor, type K F, manufactured by Sterling Electric Motors, Inc., Los Angeles, California. The over-all layout of the apparatus is shown in Figs. 1 and 2.

The mass flow of the blower was controlled by a throttle valve which was a conical block of wood attached to a threaded shaft in such a manner that turning the block would cause the block to advance toward the inlet of the blower and thereby decrease the inlet area and volume flow through the blower.

It was necessary to place a settling chamber on the exhaust side of the blower to eliminate surging in the flow. The airstream passed from the blower through a conical sheet-metal diffuser into the settling chamber which was constructed of 3/8-inch plywood and reenforced with two by fours. The external dimensions of the settling chamber were 4 feet by 4 feet by 3 feet.

After leaving the settling chamber the airstream passed through a contraction to a four-inch square duct. The contraction section was made of a pine block which was fastened to a tapering sheet metal duct; the final contraction took place through a wood fairing which was shaped so as to provide a smooth flow.

The ducts (1/4-inch plywood) were made in two sections. One section was permanently fastened to the pine contraction with extruded aluminum angles and ordinary wood screws; the removable sections were attached to the rest of the duct by extruded aluminum angles and 1/4-inch bolts.

The removable sections of the duct are shown in Fig. 3. The special section was constructed to test the effect of angle of incidence on the pressure drop across orifice plates; the slots were cut through three sides of the section, the remaining side being solid and the entire duct supported with wooden braces from beneath.

The dynamic pressure was obtained with a 1/8-inch diameter pitot-static tube which was located eight duct diameters from the contraction section and aligned with the centerline of the duct. The pressures were recorded by means of a vernier manometer. A thermometer to record the temperature of the airstream was inserted in the duct in the vicinity of the pitot tube as shown in Figs. 1 and 2.

The total pressure downstream of the orifice plate or

honeycomb grid was obtained with a 3/32-inch diameter total-head tube. The tube was located eight duct diameters downstream of the test plates and at least nine duct diameters downstream of the plates being tested at an angle of incidence to the airstream. The total pressure tubes upstream and downstream of the test specimen were connected across a U-tube manometer thus recording the drop in total head, neglecting the small duct losses due to friction.

The orifice plates, as shown in Fig. 4, were made of sheet aluminum; the holes being drilled on a drill press to the proper diameter and spaced to give the desired solidity. All burrs were removed from the holes to obtain a uniform edge condition for the holes in the various orifice plates. The test plates were bolted in position in the duct.

The honeycomb grids were made of aluminum plates; the plate thickness being varied to give the desired solidities. Sample grids are shown in Fig. 4 and a drawing of one of the grid plates is shown in Fig. 5. The plates were fitted together to form a grid; the friction between the edges of the slots in the plates and the mating plates held the grids in their form. The dimension L as shown in Fig. 5 was varied to give the desired ratio of L/D since D, the spacing of the plates in the grid, was kept constant at 1/2-inch. The honeycomb grids were held in the duct by friction.

CHAPTER III

PROCEDURE

Before any pressure drop data could be obtained, it was necessary to calibrate the duct to obtain the variation of total head and dynamic pressure in front of and behind the test section. This was done by varying the position of the pitot-static tube and total head tube in horizontal surveys across the duct for various throttle settings of the blower to obtain the variation of the pressures in the horizontal planes. The average of the values of the pressures for the surveys was then plotted versus position in the duct, and the curves were integrated to obtain the mean value of the pressure. Figs. 6 through 9 show typical variations of dynamic pressure and total head with lateral position, and Fig. 10 shows the variation of q with the pressure in the settling chamber.

It was found that the mean value of the dynamic pressure was 87 per cent of the center-line value for all throttle settings. Since the difference in total head was used, it was only necessary to take the mean value of the total head at both sections under consideration as equal to the center-line value for all throttle settings. Therefore it was necessary to record only the values of the dynamic

pressure and the total head drop for the center of the duct. The mean dynamic pressure was then 87 per cent of the recorded value and the mean total head drop was taken as being equal to the center-line value.

For each run it was necessary to record the room temperature, the temperature of the air in the duct, and the atmospheric pressure at the start and at the end of the run. The arithmetic averages of the two values were then used in the reduction of the data. Before starting a run, care was taken to align the pitot-static tube and total head tube with the center-line of the duct. The dynamic pressure and total head drop were then recorded for a series of throttle settings.

To obtain pressure-drop coefficients for orifice plates at an angle of incidence, the special section of the duct was attached directly to the permanent section and the total head tube was inserted. An orifice plate was inserted into the slot at the angle under consideration; all other slots and joints were sealed with masking tape. The dynamic pressure and total head drop were then recorded for various throttle settings and angles of incidence.

The regular section of the duct was used to obtain the pressure-drop coefficients for the honeycomb grids. The grids were inserted into the end of the duct and the ducts fastened together; the pressure drops and dynamic pressures were then recorded.

CHAPTER IV

DISCUSSION OF RESULTS

ORIFICE PLATES

Effect of Reynolds Number.--Tables 3 and 4 show the variation of the pressure-drop coefficient with Reynolds Number for orifice plates normal to the airstream and at angles of incidence to the airstream. Figs. 11 and 12 show $\Delta P/q$ plotted against Reynolds Number for the normal tests on plates of different solidities, and Fig. 13 shows $\Delta P/q$ plotted against Reynolds Number for the incidence tests with the solidity held constant. The Reynolds Number in Fig. 11 is based on W as a characteristic length, while D^2/W is the characteristic length for the Reynolds Number in Figs. 12 and 13.

It is seen from Figs. 11 and 12 that $\Delta P/q$ tends to decrease with increasing Reynolds Number to a constant value. In the normal tests for Reynolds Numbers greater than 16,000, $\Delta P/q$ is a constant for Reynolds Number greater than 10,000.

Effect of Hole Diameter, Constant Solidity.--In Figs. 11 and 12, the curves for the five orifice plates with equal values of solidity but different values of D^2/W exhibit different values of $\Delta P/q$. Fig. 14 shows the values of $\Delta P/q$ for these plates at Reynolds Numbers greater than 16,000 plotted

against the values of D^2/W. For Reynolds Number calculations the ratio of D^2/W is a characteristic dimension which was selected since it contained both the hole area, or its equivalent, D^2, and the width of the elements.

The variation of $\Delta P/q$ with D^2/W is seen to be parabolic, and there exists a value of D^2/W for which the pressure-drop coefficient will be a minimum for a given solidity.

Effect of Solidity.--To obtain the variation of the pressure-drop coefficient with solidity for orifice plates, the values of $\Delta P/q$, for Reynolds Numbers greater than 16,000, in Fig. 12 were plotted versus solidity to obtain the curve shown in Fig. 15. For the plates of equal solidity, the average value of $\Delta P/q$ was used.

When an airstream passes through the holes in an orifice plate it contracts itself so that the orifice plate will have an effective solidity that is higher than the geometric solidity. If C is the contraction ratio for the air flowing through an orifice plate, and (1-S)A is the geometric open area of the orifice plate placed transversely in a duct of area A wherein the airstream velocity is V, the velocity of the airstream at its narrowest portion can be found from the Continuity Equation. That is, since

$$\rho_1 V_1 A_1 = \rho_2 V_2 A_2$$

and if V_1 is identified with the velocity V in the duct, A_1

with the area of the duct, V_2 with the velocity at the vena contracta, and A_2 with the area at the vena contracta, then it is seen, for the incompressible case where $\rho_1 = \rho_2$, that

$$A_2 = (1-S)A_1C$$

and

$$V_2 = \frac{V_1}{(1-S)C}$$

Writing Bernoulli's Equation for the duct and the vena contracta one gets

$$P_1 + \tfrac{1}{2}\rho V_1^2 = P_2 + \tfrac{1}{2}\frac{\rho V_1^2}{(1-S)^2C^2}$$

$$P_1 - P_2 = \Delta P = \tfrac{1}{2}\rho V_1^2\left[\frac{1}{(1-S)^2C^2} - 1\right]$$

$$\frac{\Delta P}{q} + 1 = \frac{1}{(1-S)^2C^2}$$

Hydrodynamical studies show that the contraction ratio, C, for a perfect fluid passing through a single orifice in a large sheet is 0.61, O'Brien (6); so that the limiting value of $\Delta P/q$ is given by

$$\frac{\Delta P}{q} = \frac{1}{(0.61)^2(1-0)^2} - 1 = 1.69$$

The curve representing the variation of $\Delta P/q$ with solidity for a contraction ratio of 0.61 is shown in Fig. 16. It is seen that the experimental data falls below this theoretical curve.

However, the effect of increasing the diameter of a single orifice in a duct is to increase C; experimental values of C for various values of M, the ratio of orifice area to duct area, are given by O'Brien (7). Since all the air which passes through any hole of area A in a perforated sheet comes through a tube of streamlines of cross-sectional area

$$\frac{A}{1-S}$$

it is likely that the variation of C with M in a pipe is identical with the variation of C with (1-S) in the case of a flat perforated sheet. If M is identified with (1-S), it is possible to use the experimental values of C to construct an empirical curve giving $(\Delta P/q + 1)$ as a function of $1/(1-S)^2$ assuming that there is no recovery of pressure after the vena contracta. The curve obtained from the data given by O'Brien (7) is shown in Fig. 16.

It is noted that the experimental data agrees with the theoretical curve except at high solidities. The fact that the pressure-drop coefficient is found to be less than predicted by the empirical theory indicates that the pressure in the streamtubes rises after passing the vena contracta for high solidities.

If the diameter of the holes, D, of an orifice plate is of the same order of magnitude as the thickness of the

plate, as in the case of plates II and III, a flow pattern results which is different from that where D is much greater than the plate thickness. In the latter case the solid portions of the orifice plates simulate flat plates in an airstream and hence create eddies off of the edges of the solid portions; in the case of the small holes in a thick plate, the solid portions act as bluff bodies in an airstream and the resultant flow has less eddies than would be obtained with a flat plate in the same flow. One should expect a greater pressure drop across the flat-plate type orifice plate since more energy has been dissipated in creating vorticity.

Curve I in Fig. 15 shows the variation of $\Delta P/q$ with solidity for orifice plates with D of the same order of magnitude as the plate thickness. Since only two plates of this type were tested, points from work by Hoerner (2) and Taylor (4) were used to aid in the construction of the curve of experimental data. The pressure drop coefficient is lower than that for orifice plates with D large in comparison with the plate thickness.

Effect of Angle of Incidence.--The pressure loss due to an orifice plate placed obliquely in a duct, as in Fig. 13, can be calculated according to the cosine principle. The velocity can be split into a tangential and a normal component; the tangential component does not contribute to the losses

except for frictional losses, and the pressure loss of the plate corresponds to the normal component of the velocity:

$$V_N = V \cos \Lambda = V \sin \alpha$$

Since the normal component of velocity will vary as the sine of the angle of inclination, and if the dynamic pressure based on the normal component of velocity is

$$q_\alpha = \frac{\rho}{2} V_N^2 = \frac{\rho}{2} V^2 \sin^2 \alpha = q \sin^2 \alpha$$

the variation of the pressure drop coefficient is given by

$$\left(\frac{\Delta P}{q}\right)_\alpha = \left(\frac{P}{q}\right)_{\alpha = 90^\circ} \sin^2 \alpha$$

Fig. 16 shows the variation of $\Delta P/q$ with the angle of inclination as cross-plotted from Fig. 13 for Reynolds Numbers greater than 10,000. It is assumed that the effect of angle of incidence is independent of the solidity. The curve of the experimental data satisfies the theoretical relationship developed for an angle of inclination greater than thirty degrees.

At low angles of inclination the pressure-drop coefficient is greater than the theoretical result. This can be explained on the basis that the tangential component of velocity is large enough to produce a frictional loss which is no longer negligible in comparison with the pressure loss

produced by the normal component of the velocity. For the solidity tested, the variation is given by the empirical relationship

$$\left(\frac{P}{q}\right)_{\alpha} = \left(\frac{P}{q}\right)_{\alpha = 90^{\circ}} \sin^{1.75}\alpha \qquad (\alpha < 30^{\circ})$$

HONEYCOMB GRIDS

Effect of Reynolds Number.--Table 5 and Fig. 17 show the variation of the pressure-drop coefficient with Reynolds Number for the honeycomb grids; the Reynolds Number is based on W, the width of the elements of the grid. For a constant ratio of L/D and constant solidity, $\Delta P/q$ decreases rapidly with increasing Reynolds Number and approaches a constant value for Reynolds Numbers greater than 4500. The Reynolds Number for constant pressure-drop coefficient increases with increasing solidity, but more solidities must be tested before the actual variation can be determined.

Effect of Solidity.--To obtain the variation of the pressure-drop coefficient with solidity for the honeycomb grids, the values of $\Delta P/q$, for Reynolds Numbers greater than 4500 and L/D constant, in Fig. 17 were plotted versus solidity to obtain the family of curves shown in Fig. 18. The curves are similar to those in Fig. 15 for the orifice plates except that the pressure drop coefficient for the honeycomb grids does not go to zero for zero solidity.

However, one should not expect the pressure-drop coefficient to go to zero; a hypothetical honeycomb grid composed of flat plates of zero thickness would exhibit a pressure drop due to the frictional losses along the length of the plates and the interference flow in the corners. It is not advisable to extrapolate the curves of Fig. 16 to zero solidity; Pope (8) gives a value of 0.22 for a honeycomb grid with L/D of six. The exact value of the solidity is not given; nevertheless the curve in Fig. 18 apparently has a point of inflection at a solidity less than 0.089, and extrapolation of the curve is not advisable.

Effect of Fineness Ratio.--To obtain the variation of the pressure-drop coefficient with fineness ratio for the honeycomb grids, the values of $\Delta P/q$, for Reynolds Numbers greater than 4500 and constant solidity, in Fig. 17 were plotted versus L/D to obtain the family of curves shown in Fig. 19. The extrapolated values shown for values of L/D less than two are values for coarse wire screen given by Schubauer (9); it is assumed that the pressure-drop coefficient for low values of fineness ratio for a honeycomb grid will approximate the pressure-drop coefficient for a coarse wire screen.

It can be seen that for a given solidity the pressure-drop coefficient increases linearly with increasing fineness ratio at least for values of $L/D > 2$.

CHAPTER V

CONCLUSIONS AND RECOMMENDATIONS

1) The pressure-drop coefficient is a function of the dimension D^2/W for a given solidity; the variation of $\Delta P/q$ with D^2/W is approximately parabolic so that there exists a value of D^2/W such that $\Delta P/q$ is a minimum for a given solidity.

2) While practically any solidity, and hence any pressure drop, can be obtained by "corking" the holes in an orifice plate, it is shown conclusively that solidity values obtained in this manner do not result in the same pressure-drop coefficient as obtained with plates with no "corking"; that is, plates designed with the proper number of holes to obtain a desired solidity.

3) The variation of $\Delta P/q$ with solidity for an orifice plate is given, approximately, at Reynolds Numbers greater than 16,000, based on D^2/W, by

$$\frac{\Delta P}{q} = \frac{1}{(1-S)^2 C^2} - 1$$

where C is a function of the solidity, S.

4) Within the range of solidites tested, the pressure-drop coefficient is invarient for orifice plates at Reynolds

Numbers greater than 16,000 and for honeycomb grids at Reynolds Numbers greater than 4500 with constant solidity.

5) The pressure-drop coefficient variation with the angle of inclination to the airstream, for Reynolds Numbers, based on D^2/W, greater than 10,000 is given by

$$\left(\frac{\Delta P}{q}\right)_{\alpha} = \left(\frac{\Delta P}{q}\right)_{\alpha = 90^\circ} \sin^2\alpha \qquad (\alpha > 30^\circ)$$

6) For an angle of inclination less than thirty degrees experiment gives a higher value of $\Delta P/q$ than is indicated by theory; the discrepency being attributable to the frictional losses caused by the tangential component of the velocity.

7) The value of $\Delta P/q$ for a honeycomb grid increases linearly with increasing L/D for a given solidity, at least for values of $L/D > 2$.

It is recommended that research be done to determine the variation of $\Delta P/q$ with D^2/W for various solidities in order to determine $\Delta P/q$ as a function of D^2/W and S. The effect of thickness of the orifice plates on the pressure-drop coefficient should be investigated, and an empirical modification should be made to the existing theory to account for the effect of thickness and the pressure rise in the streamtubes downstream of the vena contracta.

An investigation should be made to extend the data for honeycomb grids of small plate thickness as compared to plate spacing, that is, $S << 0.10$. The circular, triangular, and other shape honeycomb grids should also be investigated.

BIBLIOGRAPHY

1- Czarnecki, K. P.; Pressure-Drop Characteristics of Orifice Plates Used to Simulate Radiators; WR L-342; Langley Field, Va.; March, 1942; pp. 1-5.

2- Hoerner, S. F. ; Pressure Losses Across Screens and Grids; A. F. Technical Report No. 6289; Wright-Patterson Air Force Base, Dayton, Ohio; November, 1950; pp. 1-7, 15.

3- O'Brien, M. P. and Hickox, G. H.; Applied Fluid Mechanics; First Edition; McGraw-Hill Book Company, Inc.; New York; 1937; pp. 162-164.

4- Taylor, G. I. and Davies, R. M.; The Aerodynamics of Porous Sheets; A. R. C. R. & M. No. 2237; London; April, 1944; pp. 8-9.

5- Schubauer, G. B., Spangenberg, W. G., and Klebanoff, P. S.; Aerodynamic Characteristics of Damping Screens; N. A. C. A. T. N. 2001; National Bureau of Standards, Washington, D. C.; January, 1950; pp. 5-8.

6- O'Brien; Op. Cit.; p. 155.

7- Ibid.; p. 165.

8- Pope, A. Y.; Wind-Tunnel Testing; John Wiley & Sons, Inc.; New York; 1947; p. 68.

9- Schubauer, G. B. and Spangenberg, W. G.; Effect of Screens in Wide-Angle Diffusers; N. A. C. A. T. N. 1610; National Bureau of Standards, Washington, D. C.; July, 1948; p. 32.

A P P E N D I X

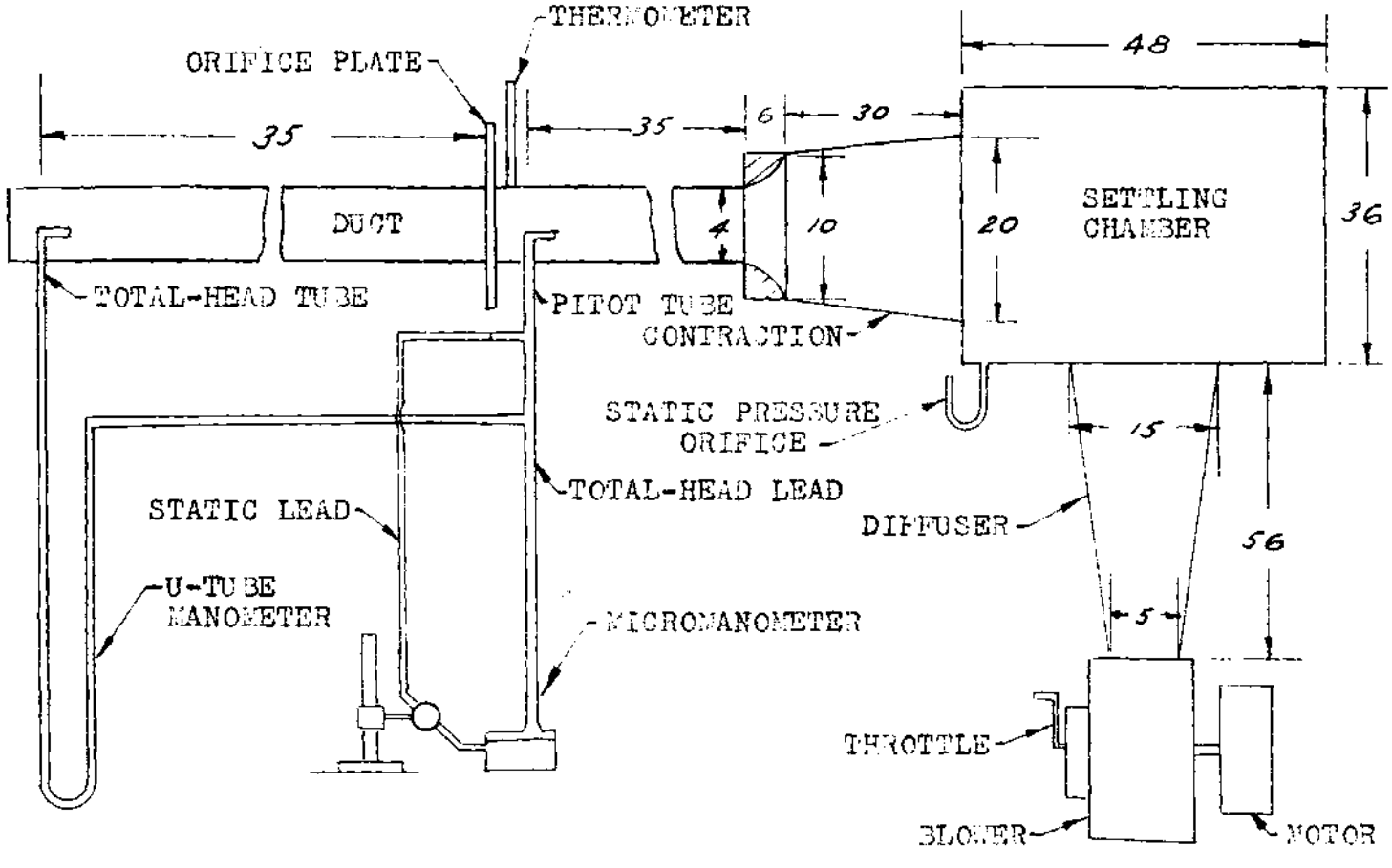

FIG. 1, SCHEMATIC LAYOUT OF APPARATUS

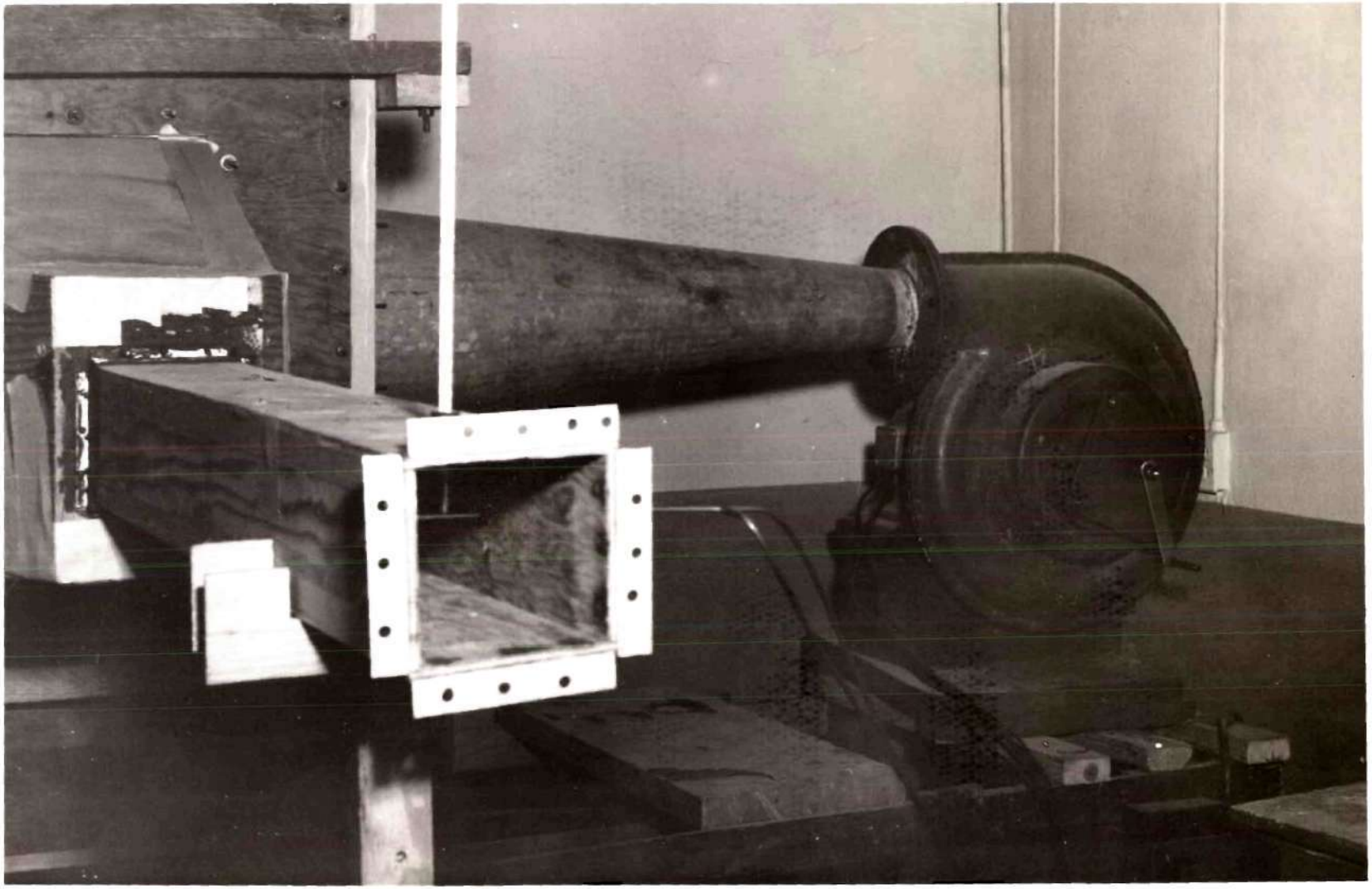

Figure 2. View of Blower and Duct.

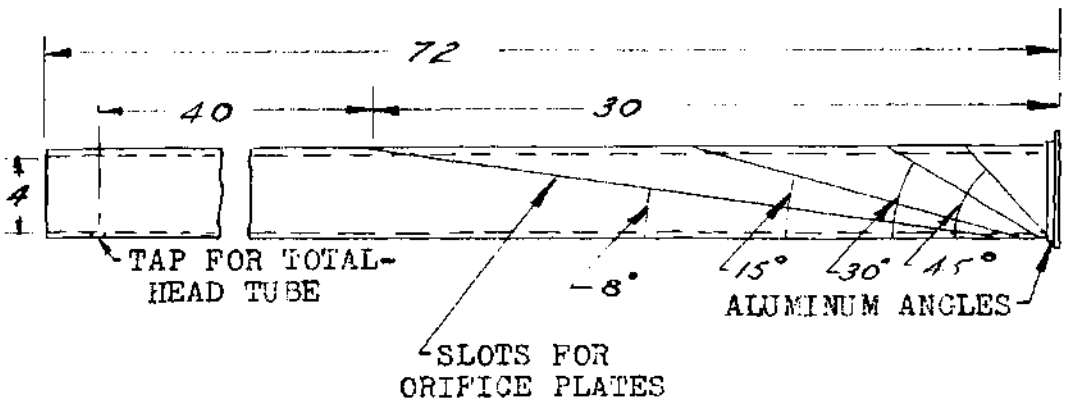

SPECIAL DUCT FOR EFFECT OF INCIDENCE

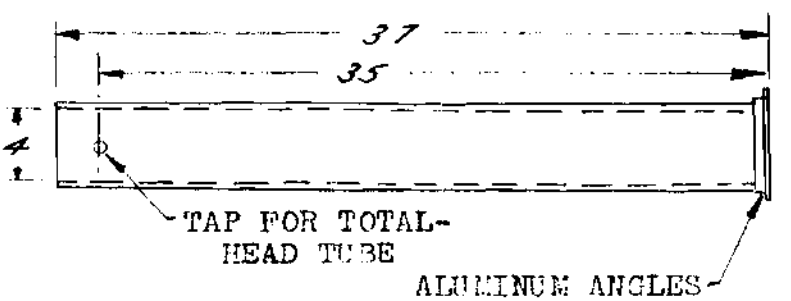

DUCT FOR ORIFICE PLATES AND HONEYCOMB GRIDS

FIG. 3, DUCT SECTIONS

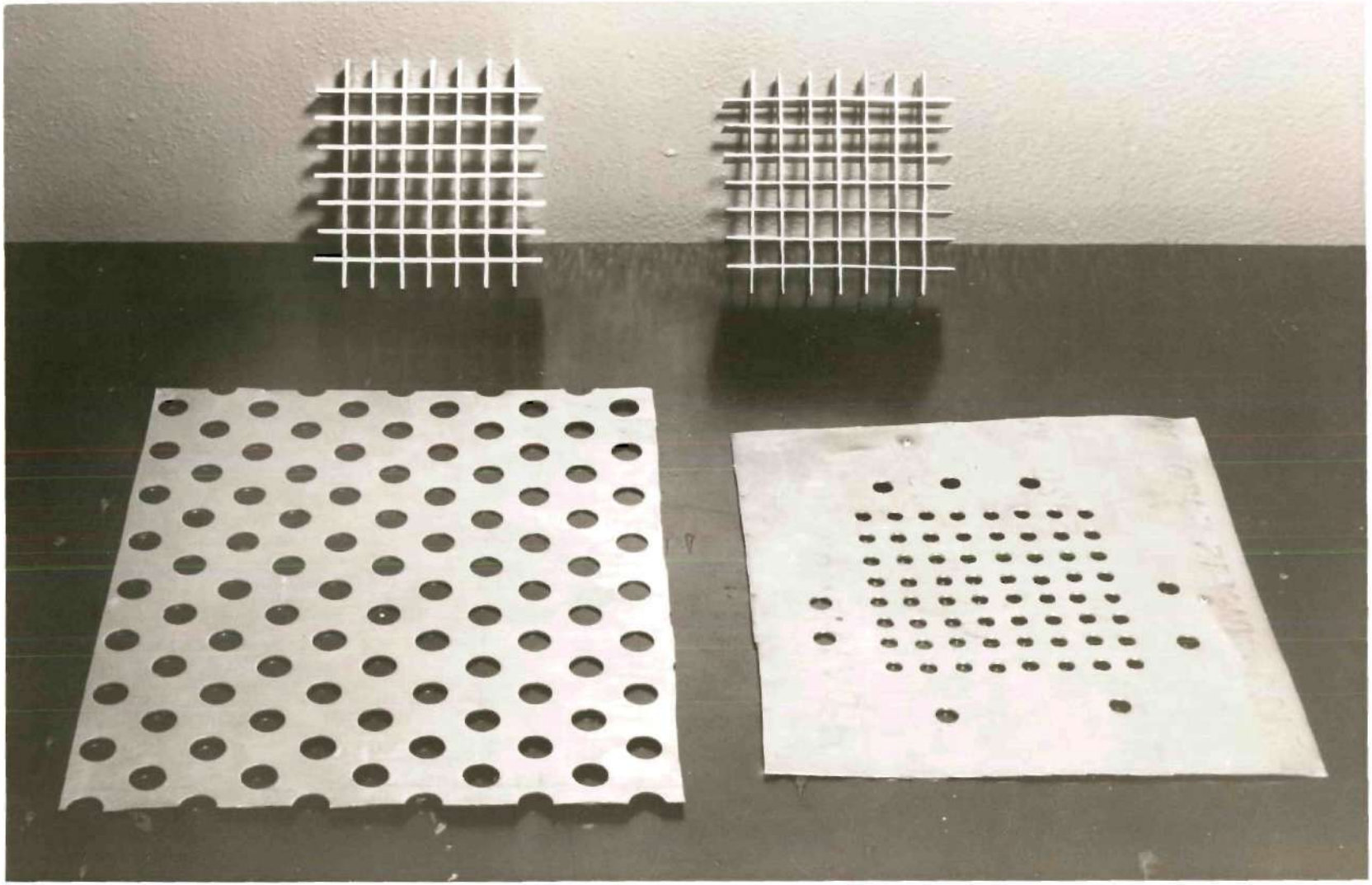

Figure 4. Sample Orifice Plates and Honeycomb Grids.

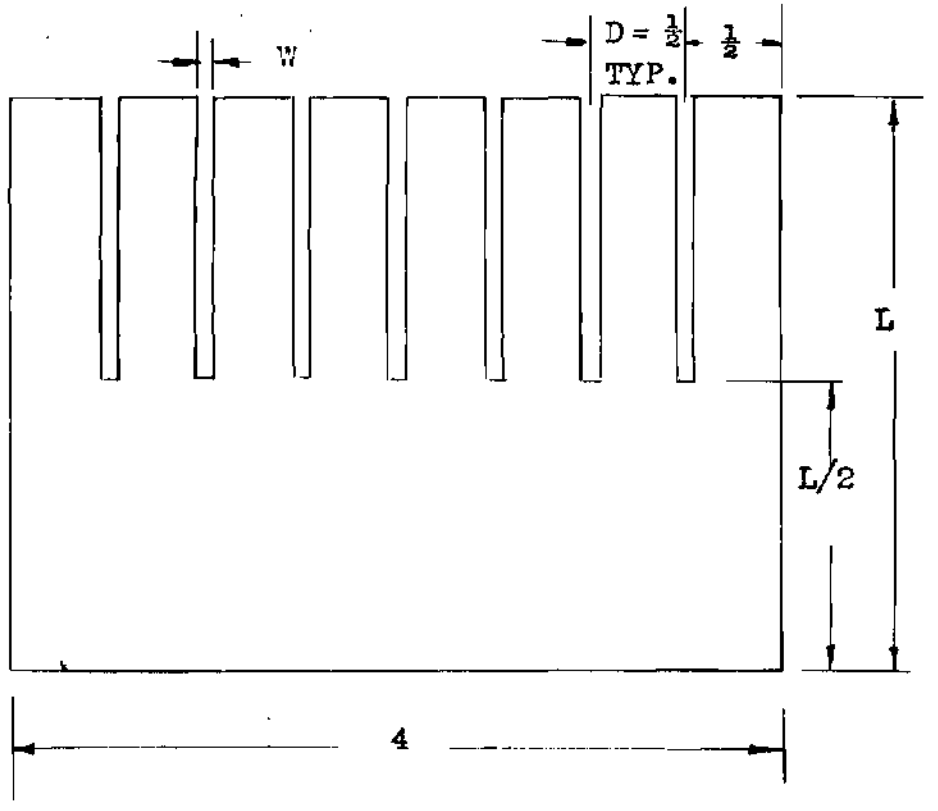

W=T=THICKNESS	0.026	0.040	0.072
S = SOLIDITY	0.089	0.135	0.236

FIG. 5, PLATE FOR HONEYCOMB GRID

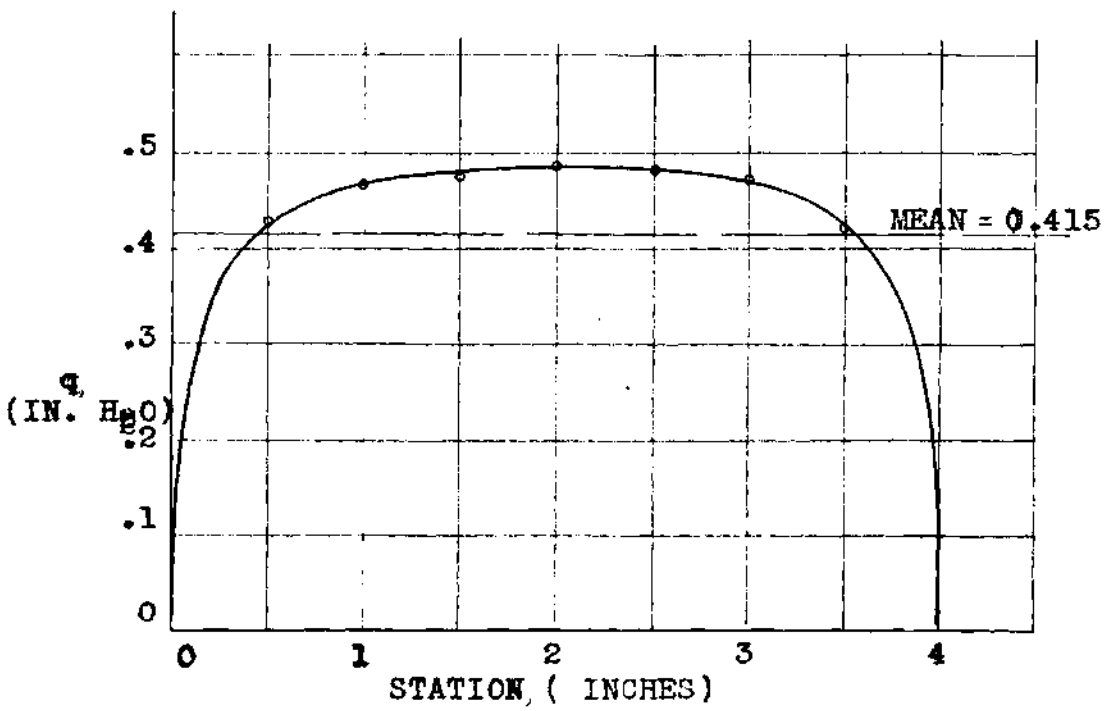

P_{SC} = 1.5 CM. ALCOHOL, DENSITY = 0.80 AT 60°F

FIG. 6, DYNAMIC PRESSURE DISTRIBUTION

UPSTREAM OF TEST SECTION

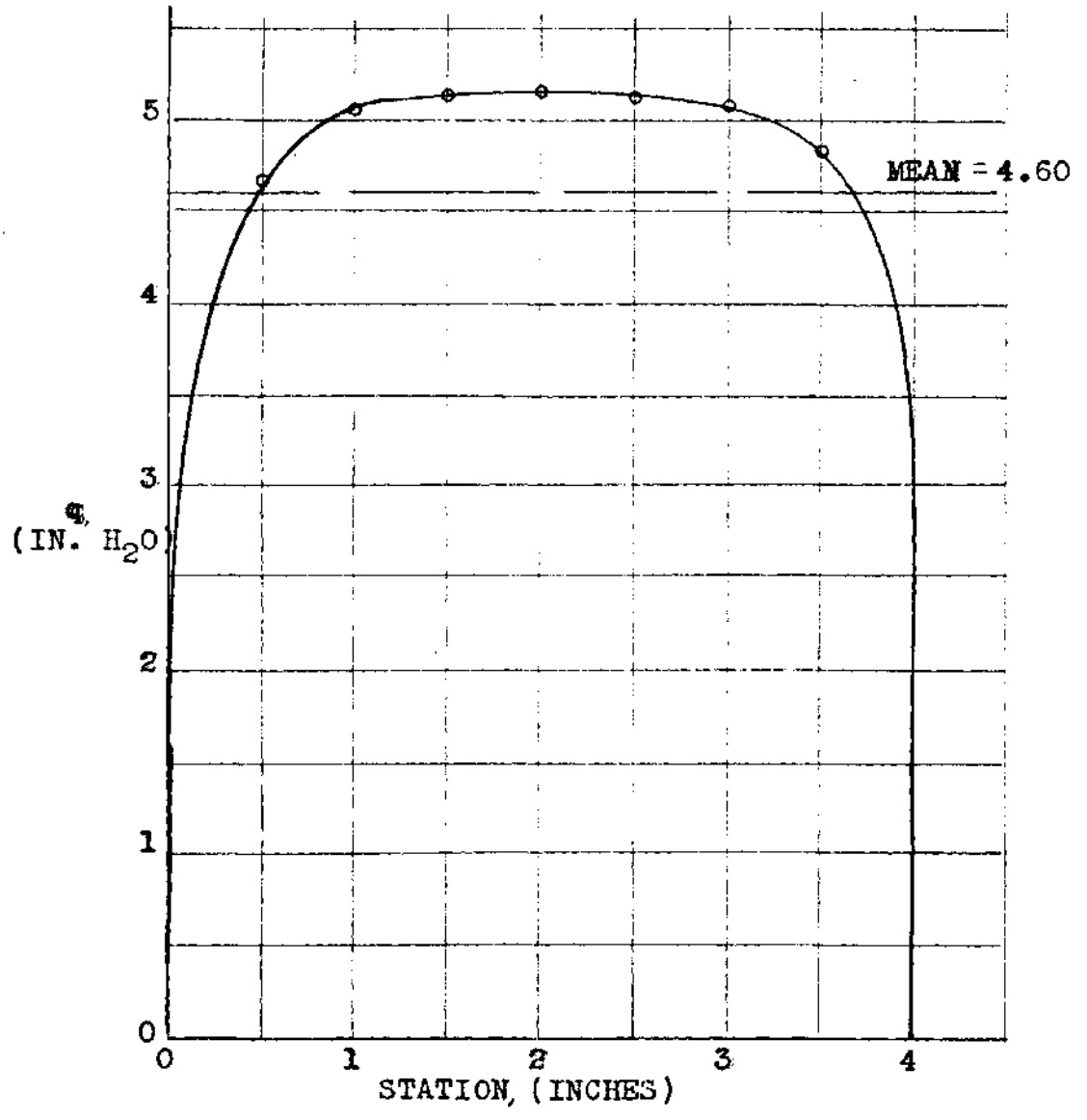

P_{SC} = 15.2 CM. ALCOHOL, DENSITY = 0.80 AT 60°F.

FIG. 7, DYNAMIC PRESSURE DISTRIBUTION

UPSTREAM OF TEST SECTION

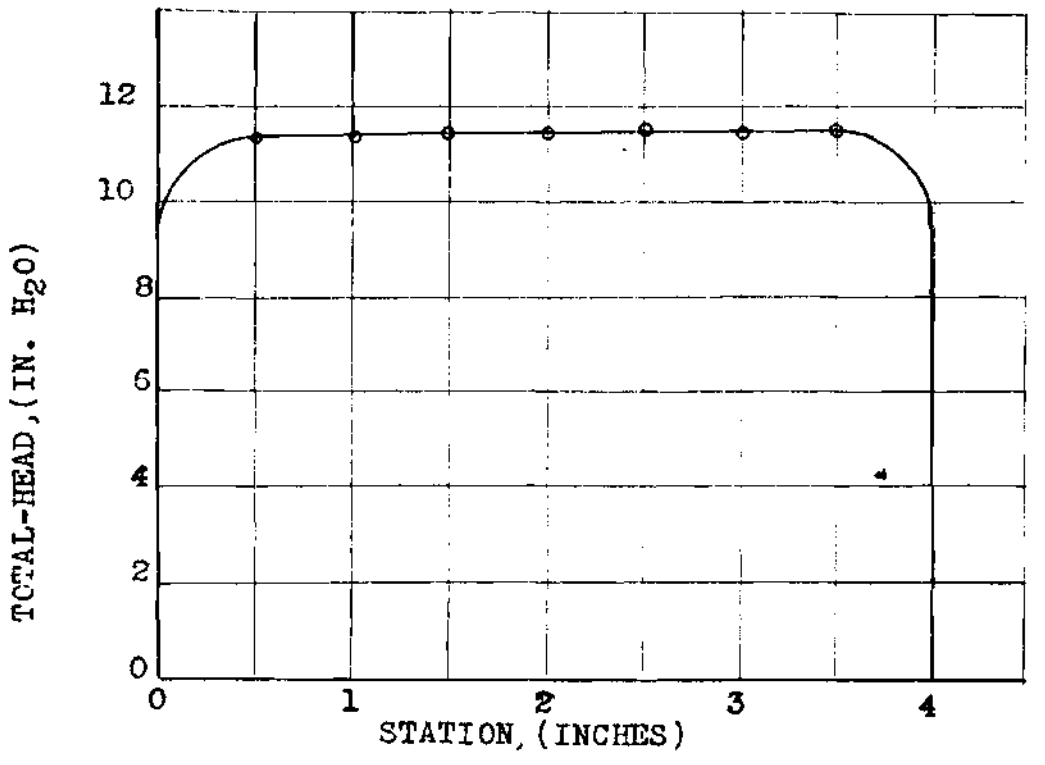

P_{SC} = 15.2 CM. ALCOHOL, DENSITY = 0.80 AT 60°F.

FIG. 8, TOTAL-HEAD DISTRIBUTION

UPSTREAM OF TEST SECTION

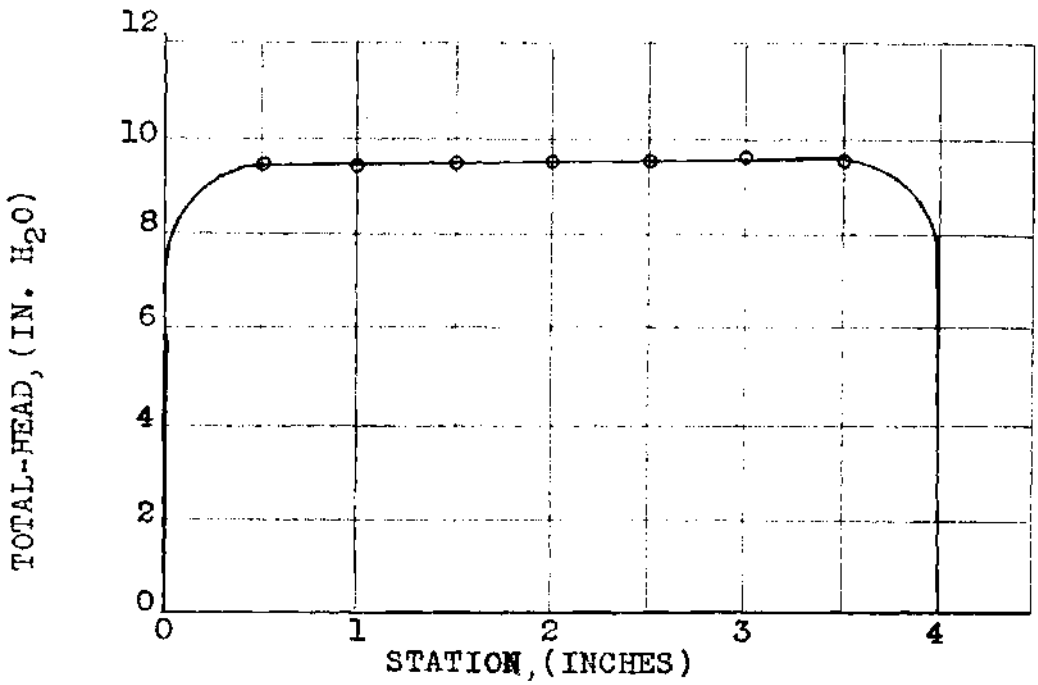

P_{SC}=15.2 CM. ALCOHOL, DENSITY = 0.80 AT 60°F.

FIG. 9, TOTAL-HEAD DISTRIBUTION

DOWNSTREAM OF TEST SECTION

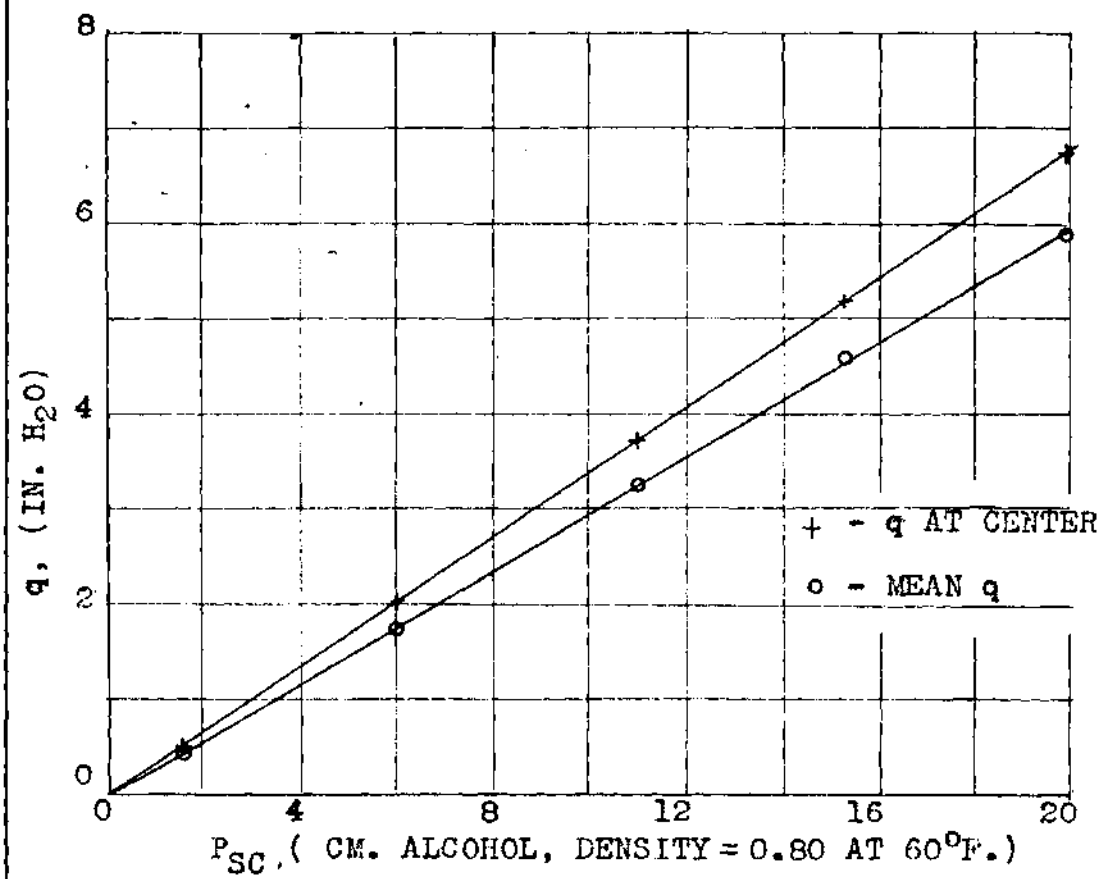

FIG. 10, VARIATION OF DYNAMIC PRESSURE UPSTREAM OF TEST SECTION WITH SETTLING CHAMBER PRESSURE

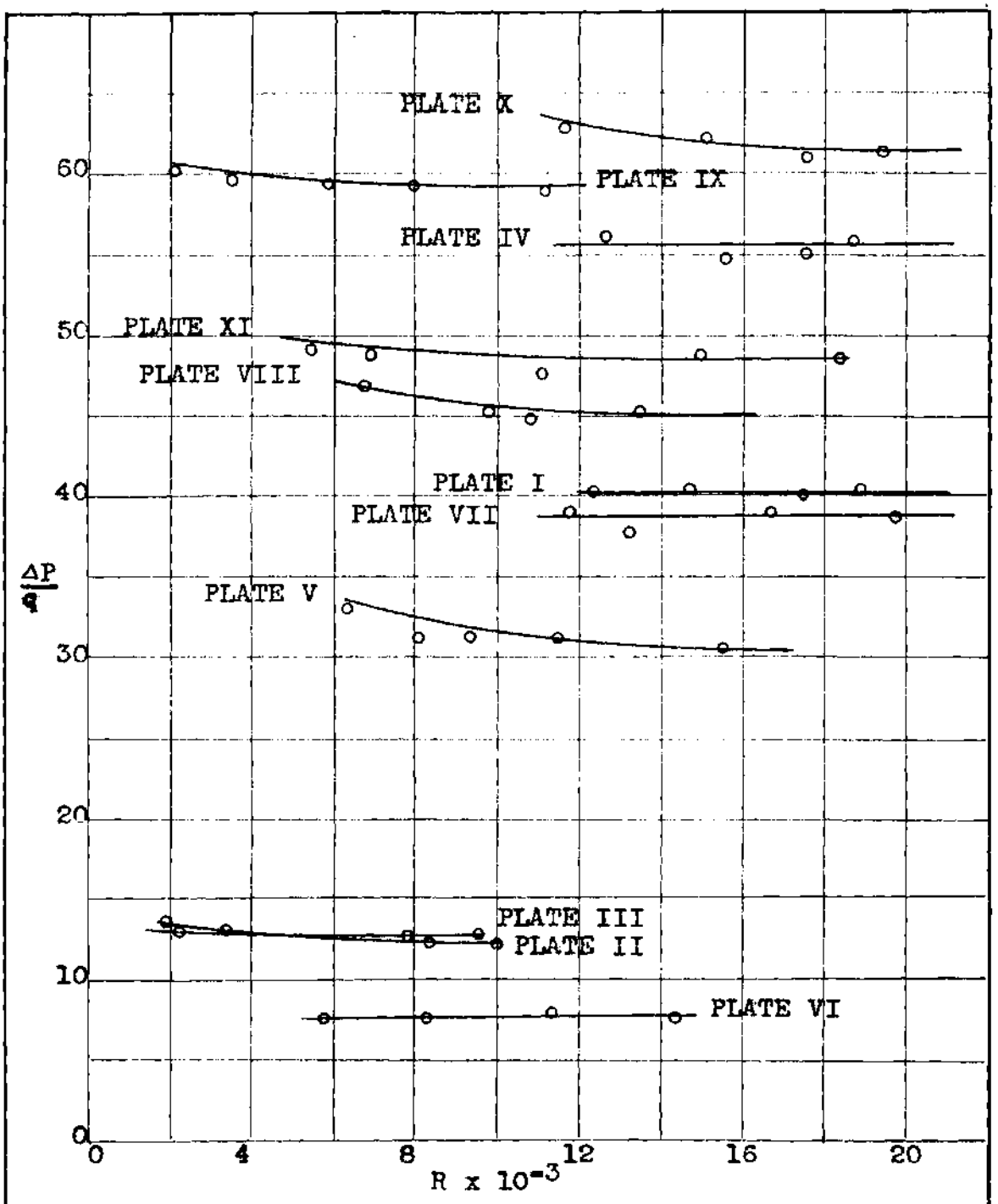

FIG. 11, VARIATION OF $\Delta P/q$ WITH REYNOLDS NUMBER BASED ON W FOR ORIFICE PLATES

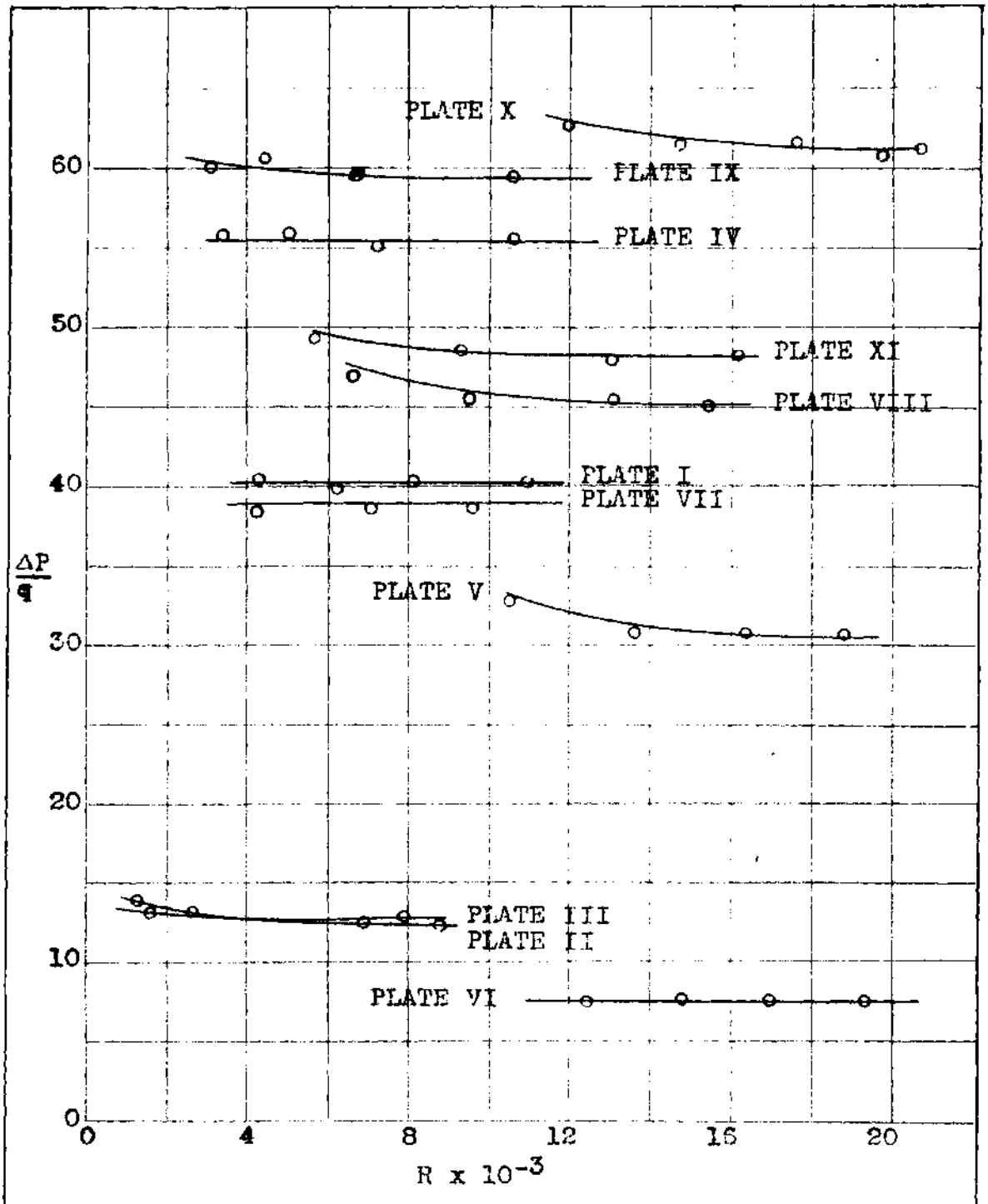

FIG. 12, VARIATION OF $\Delta P/q$ WITH REYNOLDS NUMBER BASED ON D^2/W FOR ORIFICE PLATES

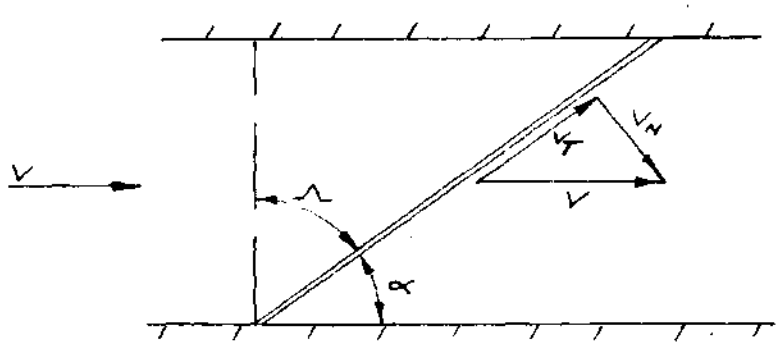

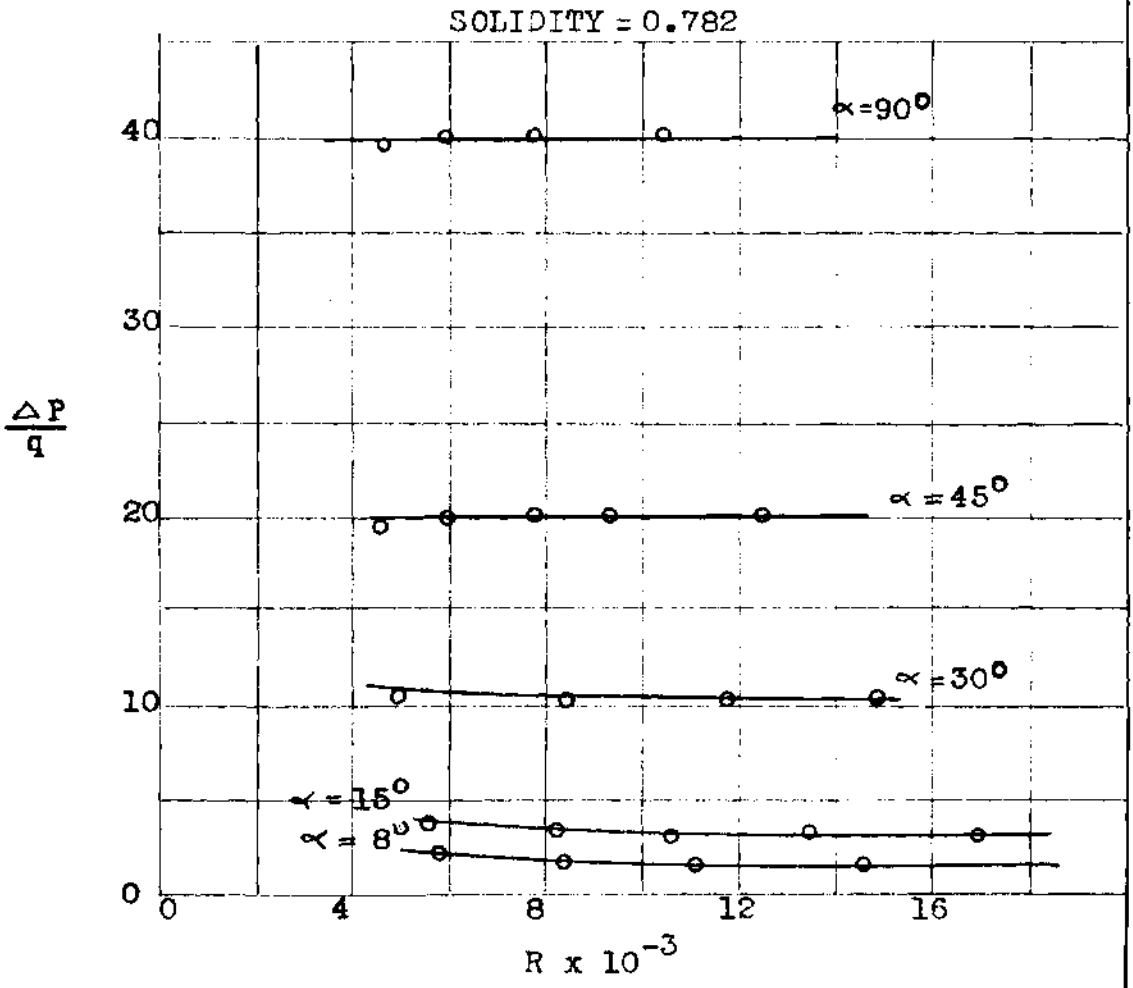

FIG. 13, VARIATION OF ΔP/q WITH R FOR ORIFICE PLATE AT DIFFERENT ANGLES OF INCLINATION

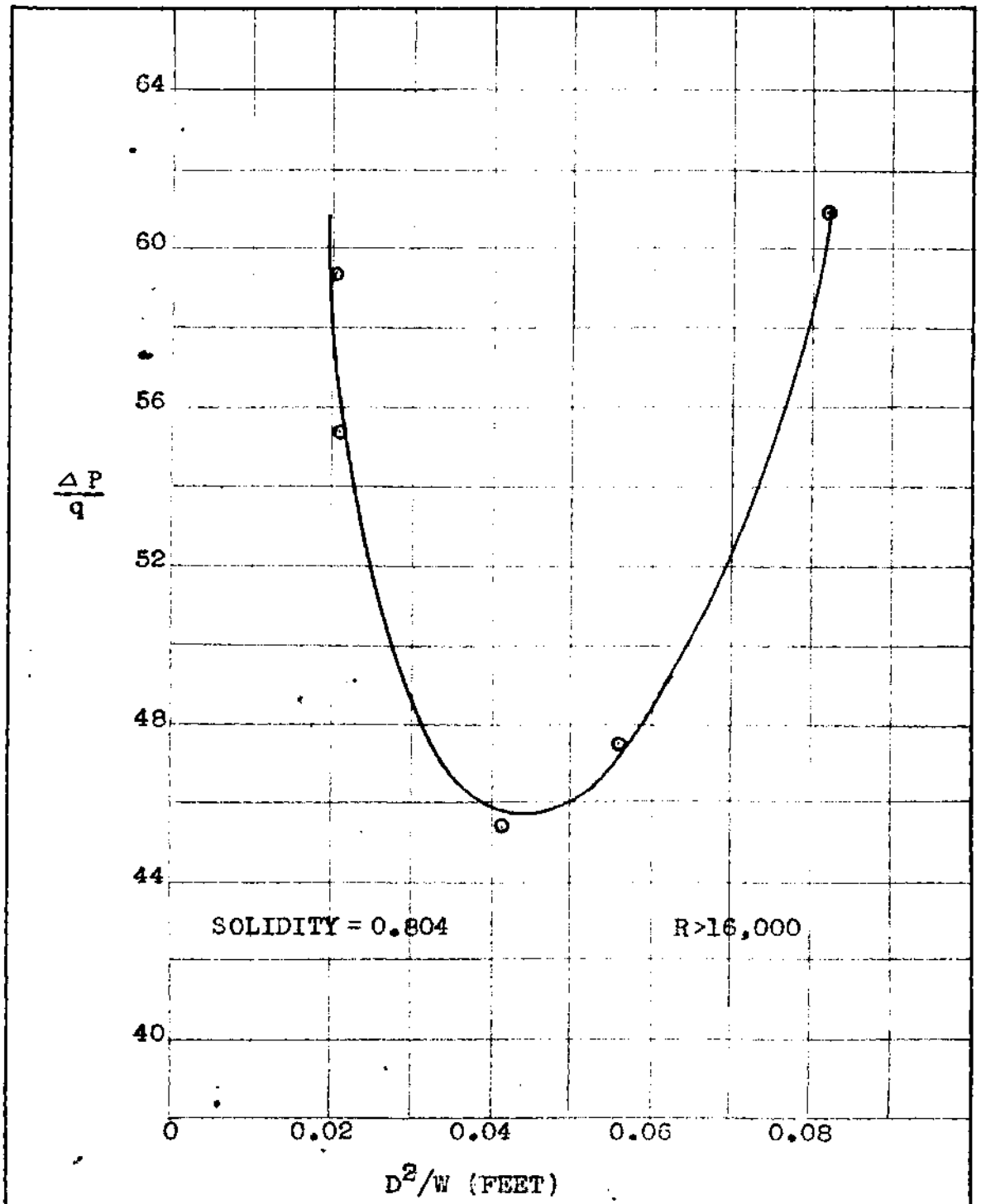

FIG. 14, VARIATION OF $\Delta P/q$ WITH D^2/W FOR CONSTANT SOLIDITY

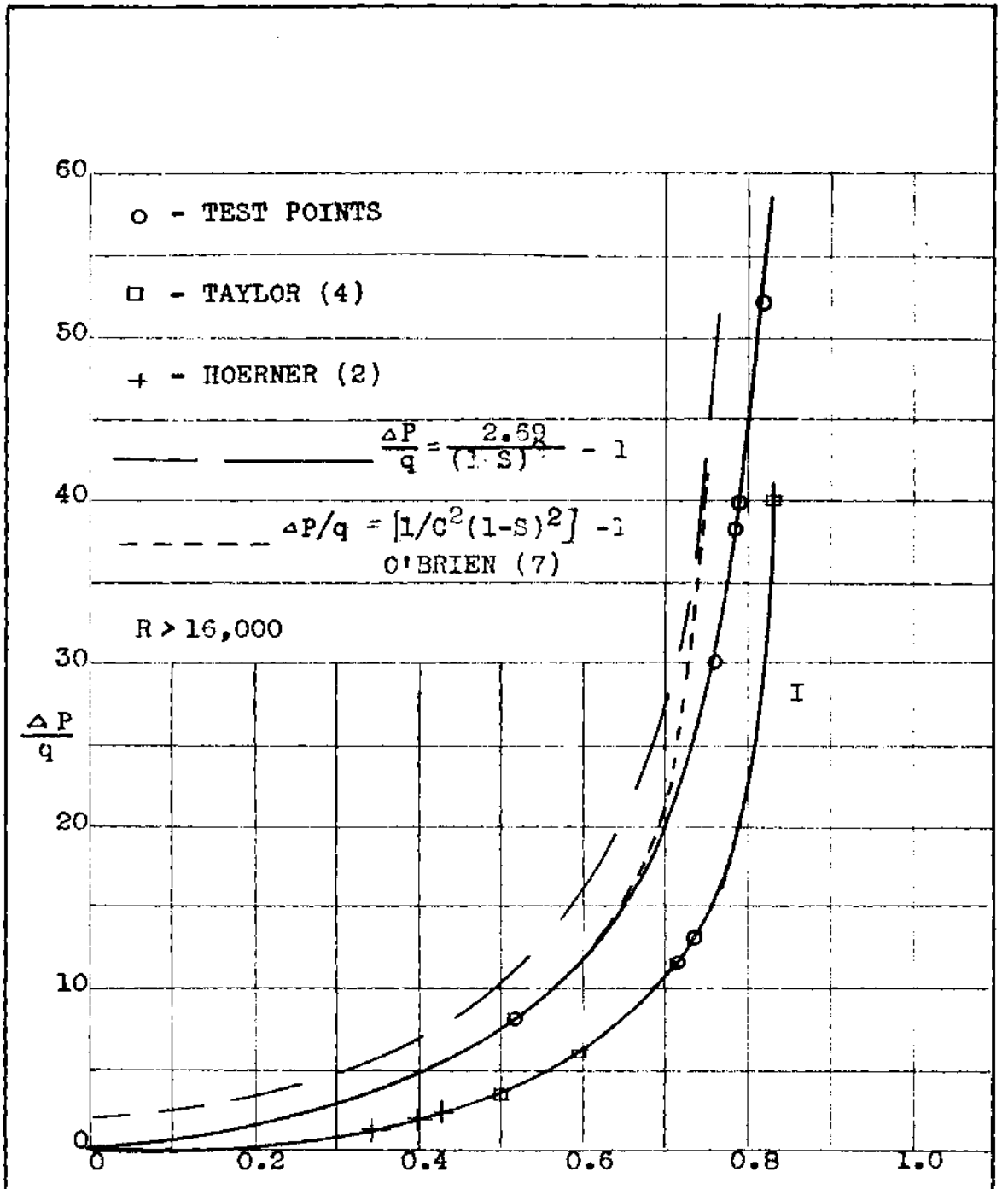

FIG. 15, VARIATION OF $\Delta P/q$ WITH SOLIDITY FOR ORIFICE PLATES

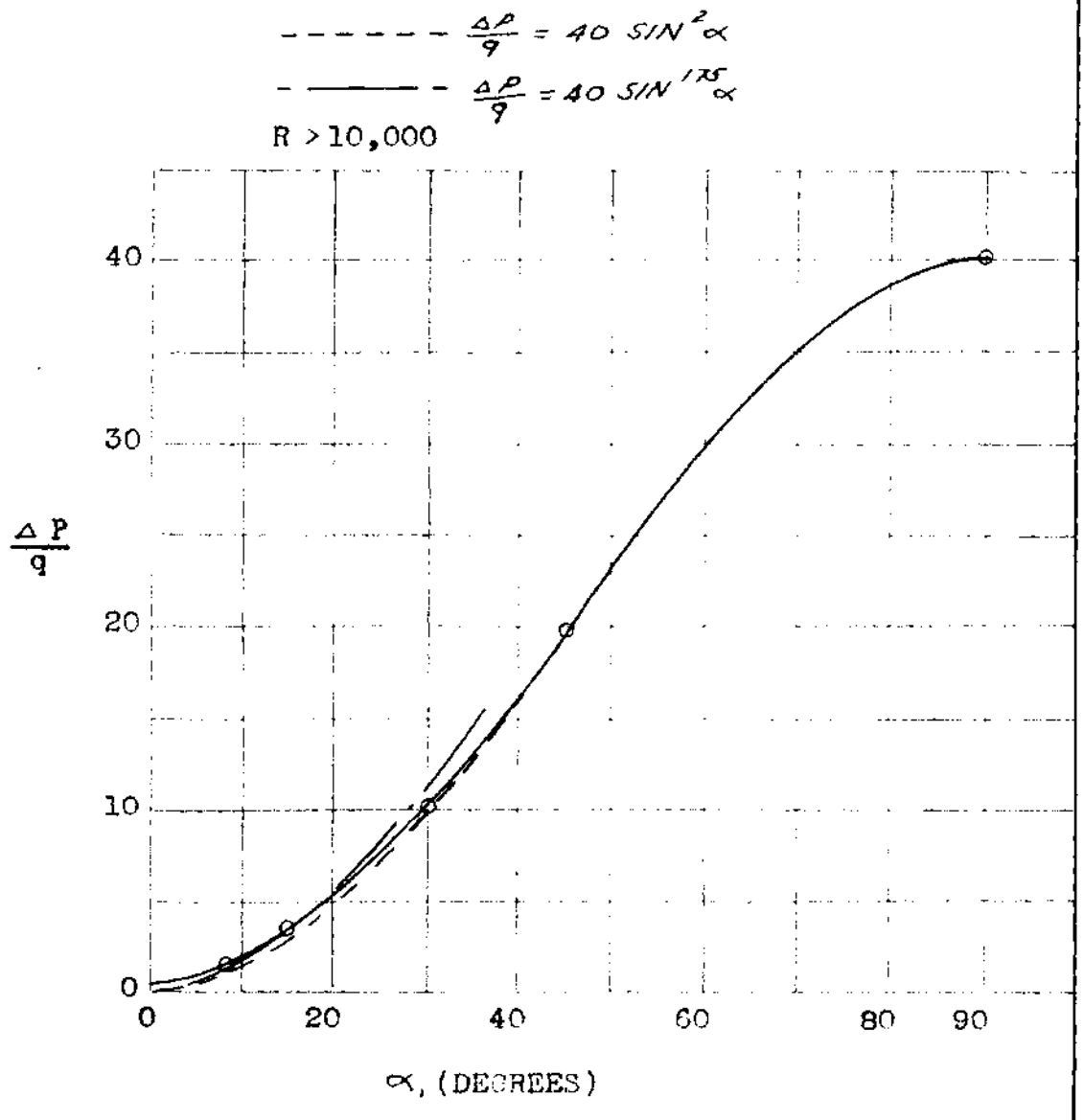

FIG. 16, EFFECT OF VARYING ANGLE OF INCLINATION OF ORIFICE PLATE

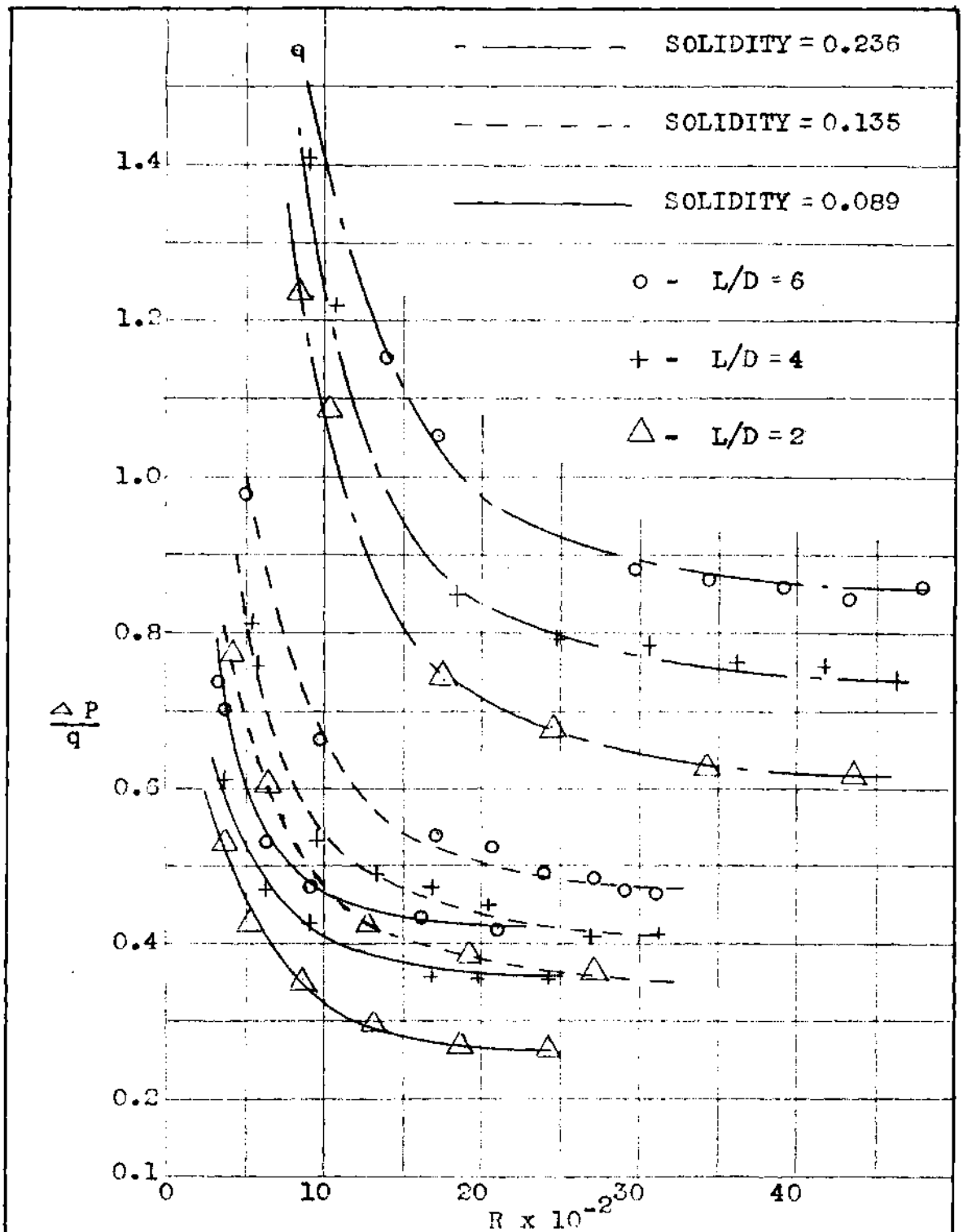

FIG. 17, VARIATION OF △P/q WITH R FOR HONEYCOMB GRIDS

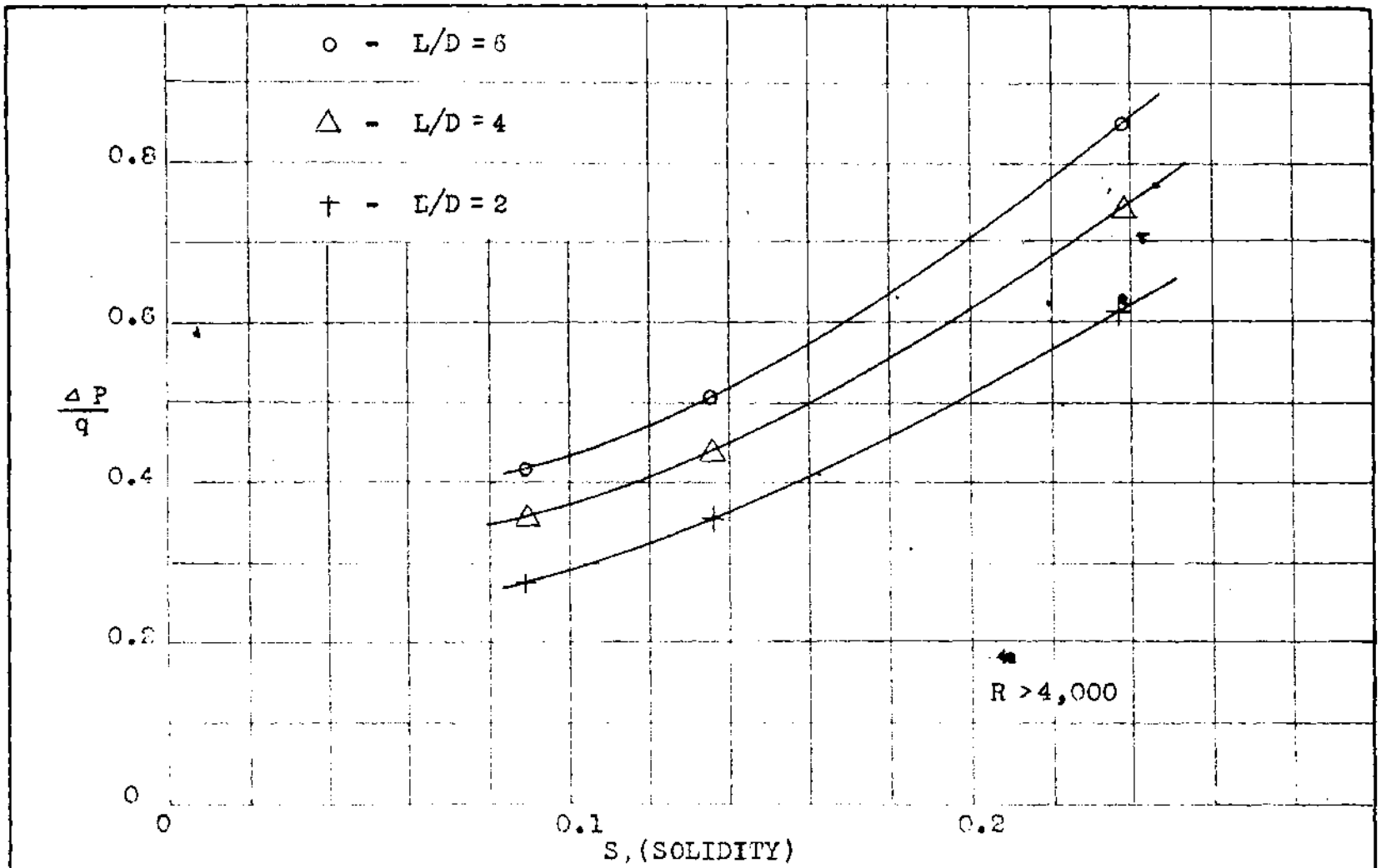

FIG. 18, VARIATION OF ΔP/q WITH S FOR HONEYCOMB GRIDS OF CONSTANT L/D

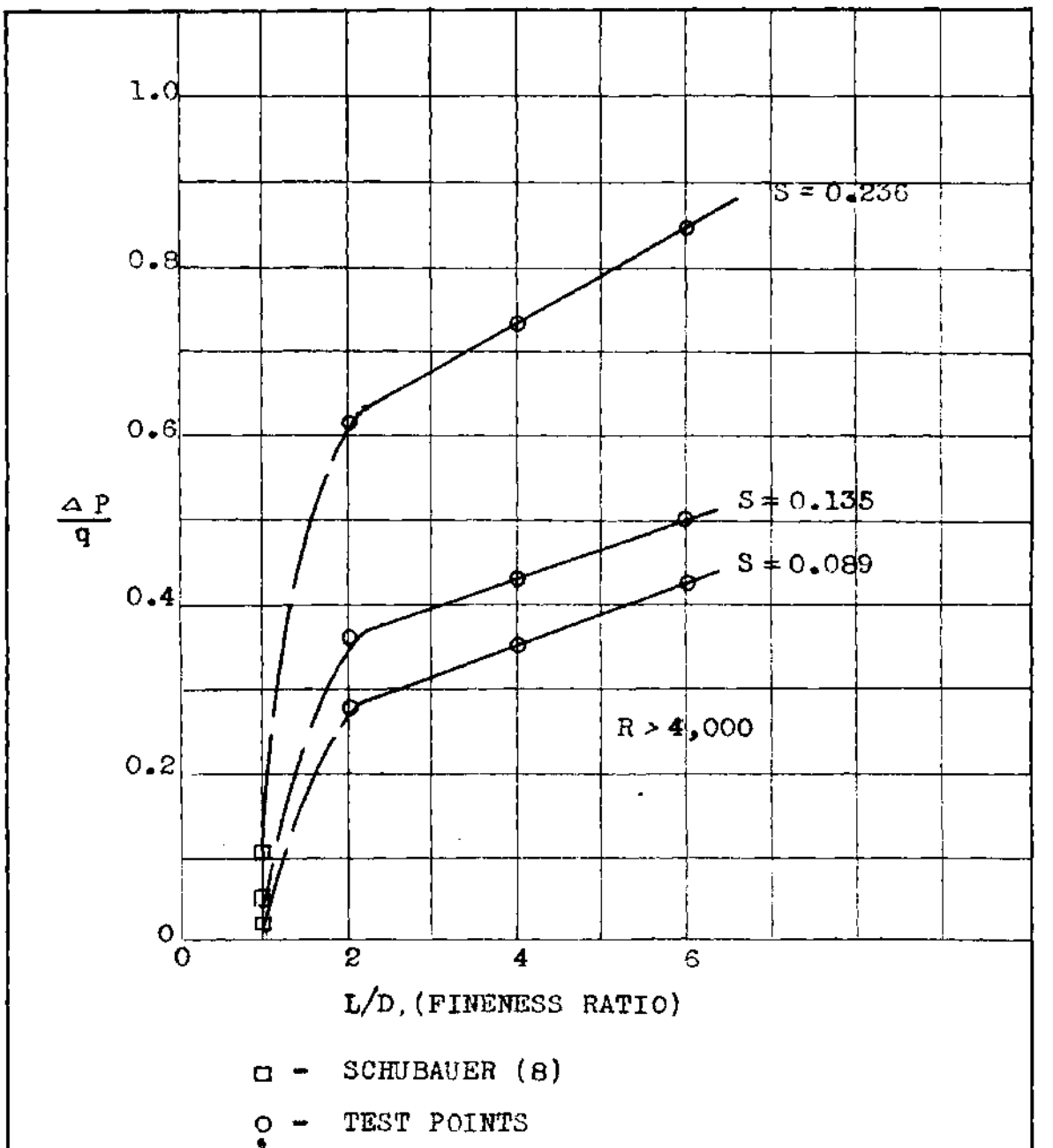

FIG. 19, VARIATION OF $\Delta P/q$ WITH L/D FOR HONEYCOMB GRIDS OF CONSTANT SOLIDITY

Table 1. Plates Tested

Plate Number	D (in.)	a (in.)	b (in.)	W (in.)	D^2/W (in.)	S	T (in.)
I	0.500	1.500	1.200	0.850	0.2940	0.782	0.040
II	0.094	0.313	0.157	0.141	0.0630	0.718	0.051
III	0.063	0.188	0.125	0.094	0.0415	0.738	0.051
IV	0.500	2.000	1.000	1.000	0.2500	0.804	0.040
V	0.563	1.000	1.000	0.437	0.7230	0.752	0.075
VI	0.500	0.938	0.688	0.313	0.7990	0.522	0.051
VII	0.531	1.969	1.000	0.954	0.2960	0.775	0.051
VIII	0.500	1.000	1.000	0.500	0.5000	0.804	0.040
IX	0.250	0.500	0.500	0.250	0.2500	0.804	0.040
X	1.000	2.000	2.000	1.000	1.0000	0.804	0.040
XI	0.672	1.344	1.344	0.672	0.6560	0.804	0.040

D- diameter of holes.

a- horizontal distance, center to center.

b- vertical distance, center to center.

W- average dimension between edges of holes; (a+b)/2-D.

S- solidity; ratio of solid area to total area.

T- plate thickness.

Table 2. Honeycomb Grids Tested

Grid Number	W (in.)	S	L/D
1	0.040	0.135	6
2	0.040	0.135	4
3	0.040	0.135	2
4	0.026	0.089	6
5	0.026	0.089	4
6	0.026	0.089	2
7	0.072	0.236	6
8	0.072	0.236	4
9	0.072	0.236	2

W- thickness of plates or width of elements.

S- solidity.

L/D- ratio of length to distance between centerlines of elements.

Table 3. Pressure-Drop Coefficient for Orifice Plates

Plate I

q (mm alcohol) density=.815	ΔP (mm alcohol) density=.815	$q' = 0.87q$	$\Delta P/q'$	q' (lb/ft^2)	V (ft/sec)	$R = \frac{\rho VW}{\mu}$	$R = \frac{\rho VD^2}{\mu W}$
6.3	213	5.5	38.8	0.91	28.3	11914	4100
10.0	347	8.7	39.8	1.45	35.8	15072	5200
12.5	445	10.9	40.8	1.82	40.2	16924	5840
14.4	509	12.5	40.7	2.08	43.0	18103	6250
15.6	556	13.6	40.8	2.26	44.8	18861	6500
16.5	589	14.4	40.8	2.39	46.1	19408	6700
17.4	619	15.2	40.7	2.53	47.4	19955	6800
18.0	635	15.7	40.5	2.61	48.1	20250	7000
18.4	660	16.0	41.1	2.68	48.7	20503	7100

Table 3. (continued)

Plate II

q (mm alcohol) density=.815	ΔP (mm alcohol) density=.815	q'=0.87q	ΔP/q'	q' (lb/ft^2)	V (ft/sec)	$R=\frac{\rho VW}{\mu}$	$R=\frac{\rho VD^2}{\mu W}$
9.5	113	8.26	13.7	1.38	34.9	2500	1100
18.5	192	16.10	11.9	2.69	48.8	3400	1500
25.6	295	22.30	13.3	3.72	57.4	4000	1760
32.8	366	28.50	12.9	4.75	64.8	4510	1990
38.4	424	33.40	12.7	5.56	70.2	4890	2150
42.3	465	36.80	12.6	6.14	73.9	5140	2260
45.0	491	39.10	12.6	6.55	76.3	5310	2340
47.4	520	41.30	12.6	6.91	78.3	5500	2420
49.0	539	42.60	12.6	7.12	79.5	5530	2430

Table 3. (continued)

Plate III

q (mm alcohol) density=.814	ΔP (mm alcohol) density=.814	q'=0.87q	$\Delta P/q'$	q' (lb/ft^2)	V (ft/sec)	$R=\frac{\rho VW}{\mu}$	$R=\frac{\rho VD^2}{\mu W}$
10.0	114	8.7	13.1	1.46	36.1	1650	740
10.1	112	8.8	12.8	1.47	36.3	1660	745
19.3	210	16.8	12.5	2.81	50.2	2290	1030
27.6	300	24.0	12.5	4.01	59.8	2730	1230
34.2	373	29.8	12.5	4.98	66.8	3050	1370
39.8	435	34.6	12.6	5.30	68.9	3140	1410
43.5	475	37.8	12.6	6.34	75.3	3430	1540
46.4	507	40.4	12.6	6.80	78.0	3560	1600
48.9	530	42.5	12.5	7.10	79.8	3640	1630

Table 3. (continued)

Plate IV

q (mm alcohol) density=.814	ΔP (mm alcohol) density=.814	q'=0.87q	$\Delta P/q'$	q' (lb/ft^2)	V (ft/sec)	$R=\frac{\rho VW}{\mu}$	$R=\frac{\rho VD^2}{\mu W}$
5.2	254	4.5	56.5	0.755	25.9	12720	3180
8.0	380	6.7	54.6	1.130	31.8	15610	3910
8.3	385	7.2	53.5	1.200	32.7	16100	4040
10.0	476	8.7	54.7	1.450	35.9	17630	4400
11.0	530	9.6	55.3	1.600	37.7	18510	4630
11.8	580	10.3	56.3	1.720	39.1	19200	4800
12.6	629	11.0	57.1	1.830	40.3	19790	4950

Table 3. (continued)

Plate V

q (mm alcohol) density=.813	ΔP (mm alcohol) density=.813	q'=0.87q	ΔP/q'	q' (lb/ft^2)	V (ft/sec)	$R=\frac{\rho VW}{\mu}$	$R=\frac{\rho VD^2}{\mu W}$
6.8	194	5.9	32.9	0.982	29.6	6280	10450
11.4	304	9.9	30.7	1.650	30.2	6400	10680
15.1	407	13.1	31.1	2.180	38.4	8140	13600
17.5	477	15.2	31.4	2.520	44.1	9350	15600
19.1	525	16.6	31.6	2.760	47.5	10070	16800
20.6	564	17.9	31.5	2.980	49.6	10520	17500
21.9	593	19.1	31.0	3.170	51.6	10940	18300
22.4	613	19.5	31.5	3.250	53.3	11300	18700
7.0	188	6.1	30.9	1.020	53.9	11430	19000

Table 3. (continued)

Plate VI

q (mm alcohol) density=.813	ΔP (mm alcohol) density=.813	q'=0.87q	$\Delta P/q'$	q' (lb/ft^2)	V (ft/sec)	$R=\frac{\rho VW}{\mu}$	$R=\frac{\rho VD^2}{\mu W}$
11.1	75.5	9.65	7.83	1.61	38.0	5810	14850
21.6	148.0	18.80	7.88	3.13	53.0	8100	20300
32.5	225.0	28.30	7.95	4.71	64.9	9930	25400
42.6	295.0	37.10	7.95	6.19	74.5	11400	29100
50.5	348.0	44.00	7.93	7.33	81.0	12400	31150
56.4	390.0	48.20	8.09	8.05	84.8	12970	32780
60.8	426.0	52.90	8.05	8.80	88.7	13570	33200
64.9	451.0	56.40	8.00	9.41	91.7	14030	33700
67.5	470.0	58.70	8.00	9.77	93.6	14320	34000
69.6	485.0	60.50	8.03	10.10	94.0	14380	35060
71.5	499.0	62.20	8.02	10.30	95.1	14550	36780
73.0	507.0	63.50	8.00	10.50	97.0	14840	37100
74.2	516.0	64.50	8.00	10.60	97.1	14850	38000

Table 3. (continued)

Plate VII

q (mm alcohol) density=.811	ΔP (mm alcohol) density=.811	q'=0.87q	$\Delta P/q'$	q' (lb/ft^2)	V (ft/sec)	$R=\frac{\rho VW}{\mu}$	$R=\frac{\rho VD^2}{\mu W}$
6.5	213	5.65	37.8	0.94	29.2	13290	4130
10.2	347	8.90	39.0	1.47	36.5	16610	5160
13.0	441	11.30	39.1	1.87	41.3	18790	5850
14.6	502	12.70	39.2	2.11	43.8	19930	6200
16.4	520	14.30	36.5	2.37	47.4	21570	6700
17.1	586	14.90	39.3	2.47	47.7	21700	6750
17.5	611	15.20	40.1	2.52	48.5	22070	6850

Table 3. (continued)

Plate VIII

q (mm alcohol) density=.811	ΔP (mm alcohol) density=.811	q'=0.87q	$\Delta P/q'$	q' (lb/ft^2)	V (ft/sec)	$R=\frac{\rho VW}{\mu}$	$R=\frac{\rho VD^2}{\mu W}$
5.2	211	4.50	46.9	0.747	26.0	6210	6210
8.7	338	7.56	44.7	1.250	33.7	8050	8050
11.2	442	9.75	45.4	1.640	38.6	9230	9230
13.2	500	11.50	43.5	1.910	41.6	9940	9940
13.7	549	11.90	46.1	1.970	42.2	10090	10090
15.0	581	13.10	44.4	2.170	44.4	10610	10610
15.4	608	13.40	45.4	2.230	45.0	10760	10760
16.0	627	13.90	45.1	2.300	45.6	10900	10900

Table 3. (continued)

Plate IX

q (mm alcohol) density=.811	ΔP (mm alcohol) density=.811	q'=0.87q	$\Delta P/q'$	q' (lb/ft^2)	V (ft/sec)	$R=\frac{\rho VW}{\mu}$	$R=\frac{\rho VD^2}{\mu W}$
4.8	242	4.17	58.0	0.691	25.1	3010	3010
5.0	251	4.35	57.8	0.720	25.6	3070	3070
7.4	369	6.44	57.4	1.070	31.1	3730	3730
8.7	462	7.56	61.1	1.260	33.8	4060	4060
10.1	522	8.80	59.4	1.460	36.5	4380	4380
11.0	564	9.56	59.1	1.590	37.9	4550	4550
11.2	594	9.75	60.9	1.620	38.4	4610	4610
11.5	614	10.00	61.4	1.660	38.8	4660	4660

Table 3. (continued)

Plate X

q (mm alcohol) density=.806	ΔP (mm alcohol) density=.806	q'=0.87q	$\Delta P/q'$	q' (lb/ft^2)	V (ft/sec)	$R=\frac{\rho VW}{\mu}$	$R=\frac{\rho VD^2}{\mu W}$
4.6	251	4.00	62.9	0.660	24.3	11710	11710
7.3	393	6.35	61.8	1.050	30.6	14750	14750
9.1	479	7.91	60.6	1.310	34.3	16530	16530
10.2	536	8.87	60.5	1.460	36.2	17450	17450
11.1	582	9.66	60.3	1.600	37.9	18270	18270
11.6	611	10.10	60.3	1.660	38.5	18560	18560
12.0	635	10.40	61.0	1.720	39.2	18890	18890
12.5	665	10.90	61.0	1.800	40.1	19330	19330

Table 3. (continued)

Plate XI

q (mm alcohol) density=.803	ΔP (mm alcohol) density=.803	$q'=0.87q$	$\Delta P/q'$	q' (lb/ft^2)	V (ft/sec)	$R=\frac{\rho VW}{\mu}$	$R=\frac{\rho VD^2}{\mu W}$
2.4	103.3	2.1	49.5	0.345	17.6	5460	5460
3.8	162.5	3.3	49.0	0.541	22.1	6860	6860
7.0	298.0	6.1	48.8	1.000	30.0	9330	9330
9.9	407.0	8.6	47.6	1.410	35.6	11100	11100
11.7	483.0	10.2	47.3	1.675	38.9	12100	12100
12.6	533.0	11.0	48.3	1.810	40.4	12550	12550
13.7	572.0	12.0	47.5	1.970	42.1	13100	13100

Table 4. Effect of Angle of Incidence on Pressure-Drop Coefficient

Plate I--8°

q (mm alcohol) density=.808	ΔP (mm alcohol) density=.808	q'=0.87q	$\Delta P/q'$	q' (lb/ft^2)	V (ft/sec)	$R = \frac{\rho V D^2}{\mu W}$
12.9	25.2	11.2	2.25	1.85	40.6	5795
27.3	50.4	23.7	2.13	3.92	59.1	8435
45.6	81.5	39.6	2.06	6.55	76.5	10920
64.6	115.0	56.1	2.04	9.30	91.0	12990
82.6	143.0	71.9	1.99	11.90	103.0	14700
99.0	171.0	86.1	1.98	14.25	113.0	16130
113.0	197.0	98.4	2.00	16.30	121.0	17280
125.6	218.0	109.1	2.00	18.10	127.0	18120
137.8	234.0	120.0	1.95	19.85	133.0	18980
143.9	248.0	125.6	1.97	20.80	136.0	19410
150.4	259.0	131.0	1.97	21.70	139.0	19840
156.9	268.0	136.5	1.97	22.60	144.0	20550

Table 4. (continued)

Plate I--15°

q (mm alcohol) density=.808	ΔP (mm alcohol) density=.808	q'=0.87q	$\Delta P/q'$	q' (lb/ft^2)	V (ft/sec)	$R=\frac{\rho VD^2}{\mu W}$
11.2	38.2	9.7	3.94	1.61	37.9	5410
24.6	79.4	21.4	3.71	3.54	56.2	8020
40.0	124.0	34.8	3.56	5.77	71.7	10230
56.4	176.0	49.1	3.58	8.11	84.9	12120
68.5	213.0	59.6	3.57	9.88	93.7	13370
81.8	253.0	71.2	3.55	11.81	102.5	14630
91.6	284.0	79.7	3.56	13.21	108.2	15440
99.4	306.0	86.5	3.54	14.30	112.8	16100
106.1	328.0	92.3	3.55	15.29	115.8	16530
111.6	342.0	97.1	3.52	16.07	120.0	17130
117.0	356.0	101.8	3.49	16.85	122.5	17480
120.1	366.0	104.5	3.50	17.26	124.0	17700
123.4	373.0	107.4	3.47	17.78	126.0	17980

Table 4. (continued)

Plate I--30°

q (mm alcohol) density=.808	ΔP (mm alcohol) density=.808	q'=0.87q	ΔP/q'	q' (lb/ft^2)	V (ft/sec)	$R=\frac{\rho VD^2}{\mu W}$
9.3	86.5	8.1	10.7	1.34	34.5	4920
18.3	163.0	15.9	10.3	2.64	58.7	8380
26.9	246.0	23.4	10.5	3.87	67.0	9560
34.9	318.0	30.4	10.4	5.04	72.3	10320
40.8	376.0	35.5	10.6	5.89	76.6	10930
45.7	417.0	39.8	10.5	6.58	79.6	11360
49.6	453.0	43.1	10.5	7.14	82.0	11700
52.5	478.0	45.6	10.5	7.55	83.0	11850
53.9	499.0	46.9	10.6	7.76	84.8	12100

Table 4. (continued)

Plate I--45°

q (mm alcohol) density=.807	ΔP (mm alcohol) density=.807	q'=0.87q	ΔP/q'	q' (lb/ft^2)	V (ft/sec)	$R=\frac{\rho VD}{\mu W}^2$
7.6	132	6.6	20.0	1.09	31.3	4470
13.4	239	11.7	20.2	1.93	41.5	5920
19.0	339	16.5	20.2	2.72	49.4	7050
23.0	410	20.0	20.2	3.30	54.3	7750
26.1	468	22.7	20.3	3.75	57.9	8260
28.6	509	24.9	20.2	4.10	60.5	8640
30.0	536	26.1	20.2	4.30	62.0	8850
31.1	560	27.0	20.2	4.45	63.1	9000

Table 5. Pressure-Drop Coefficients for Honeycomb Grids

Grid I

q (mm alcohol) density=0.813	ΔP (mm alcohol) density=0.813	q'=0.87q	$\Delta P/q'$	q' (lb/ft^2)	V (ft/sec)	$R=\frac{\rho VW}{\mu}$
6.4	5.05	5.6	0.904	0.933	28.5	573
17.6	10.10	15.3	0.660	2.541	47.1	947
36.0	18.10	31.3	0.578	5.210	67.4	1355
57.8	27.20	50.0	0.544	8.310	85.2	1713
83.0	38.30	72.2	0.531	12.000	102.2	2054
107.4	46.30	93.5	0.495	15.580	116.5	2340
131.4	56.40	114.5	0.492	19.040	129.0	2590
151.2	64.40	131.8	0.489	21.900	138.3	2780
166.6	68.40	145.0	0.471	24.100	145.0	2910
182.1	72.50	158.3	0.457	26.350	151.5	3050
194.7	84.60	169.3	0.499	28.200	156.9	3150
206.6	86.60	179.9	0.482	29.900	161.5	3250

Table 5. (continued)

Grid II

q (mm alcohol) density=0.812	ΔP (mm alcohol) density=0.812	q'=0.87q	ΔP/q'	q' (lb/ft^2)	V (ft/sec)	$R=\frac{\rho VW}{\mu}$
6.0	4.00	5.2	0.770	0.864	27.5	546
17.3	8.05	15.1	0.533	2.510	47.0	934
35.4	15.10	30.8	0.491	5.120	67.0	1330
56.1	23.20	48.9	0.474	8.130	84.5	1680
80.7	31.20	70.2	0.444	11.680	101.5	2020
106.3	39.30	92.5	0.426	15.390	116.3	2310
129.1	48.30	112.3	0.430	18.700	128.1	2550
147.4	52.30	128.2	0.407	21.300	136.8	2720
165.3	59.30	144.0	0.411	23.950	145.0	2880
180.4	63.40	157.0	0.403	26.100	151.5	3010
194.0	67.40	169.0	0.399	28.100	157.0	3120

Table 5. (continued)

Grid III

q (mm alcohol) density=0.812	ΔP (mm alcohol) density=0.812	q'=0.87q	ΔP/q'	q' (lb/ft^2)	V (ft/sec)	$R=\frac{\rho VW}{\mu}$
5.6	4.00	4.9	0.816	0.814	26.8	531
16.9	8.05	14.7	0.548	2.440	46.3	918
35.0	15.10	30.5	0.496	5.080	66.8	1320
57.0	23.10	49.6	0.466	8.240	85.3	1690
80.1	29.20	69.6	0.420	11.570	101.0	2000
107.6	40.30	93.6	0.430	15.580	117.0	2320
131.4	48.30	111.4	0.434	18.500	127.6	2530
150.8	55.40	131.1	0.423	21.800	138.5	2750
165.2	61.40	144.0	0.426	23.900	145.0	2880
183.2	69.40	159.6	0.436	26.500	152.8	3030
197.4	75.50	171.8	0.439	28.500	158.1	3140

Table 5. (continued)

Grid IV

q (mm alcohol) density=0.812	ΔP (mm alcohol) density=0.812	$q'=0.87q$	$\Delta P/q'$	q' (lb/ft^2)	V (ft/sec)	$R=\frac{\rho VW}{\mu}$
6.5	4.00	5.7	0.703	0.946	28.8	372
17.4	8.05	15.2	0.529	2.520	47.0	607
34.3	14.10	29.8	0.474	4.940	65.8	850
56.1	22.20	48.8	0.456	8.100	84.5	1090
80.7	32.20	70.3	0.458	11.680	101.0	1300
106.0	40.20	92.2	0.436	15.300	116.1	1500
129.1	49.30	112.3	0.439	18.640	128.0	1650
146.4	57.30	127.3	0.449	21.150	136.3	1760
165.0	64.40	143.6	0.449	23.800	144.8	1870
180.6	70.40	152.1	0.463	25.250	149.0	1920

Table 5. (continued)

Grid V

q (mm alcohol) density=0.814	ΔP (mm alcohol) density=0.814	q'=0.87q	ΔP/q'	q' (lb/ft^2)	V (ft/sec)	$R=\frac{\rho VW}{\mu}$
5.6	3.00	4.9	0.613	0.816	26.8	347
17.3	7.04	15.1	0.466	2.520	47.1	610
35.6	13.10	31.0	0.424	5.160	67.3	870
59.4	21.20	51.6	0.411	8.600	87.0	1130
83.5	27.20	72.6	0.374	12.100	103.0	1330
108.1	35.20	94.0	0.374	15.700	117.4	1520
131.2	41.20	114.1	0.361	19.000	129.4	1680
149.1	49.30	130.0	0.378	21.700	138.1	1790
167.4	52.30	145.8	0.360	24.300	146.1	1890
183.2	56.30	159.6	0.353	26.600	153.0	1980
199.3	61.40	173.5	0.353	28.900	159.0	2060

Table 5. (continued)

Grid VI

q (mm alcohol) density=0.813	ΔP (mm alcohol) density=0.813	q'=0.87q	ΔP/q'	q' (lb/ft^2)	V (ft/sec)	$R=\frac{\rho VW}{\mu}$
6.4	3.02	5.6	0.539	0.931	28.6	370
17.3	5.03	15.1	0.433	2.510	46.9	606
35.9	11.10	31.2	0.355	5.190	67.5	873
57.0	17.10	49.6	0.345	8.250	85.2	1100
80.2	21.20	69.6	0.345	11.580	101.0	1310
106.6	27.20	92.6	0.297	15.400	116.2	1500
131.7	31.20	114.6	0.273	19.050	129.2	1670
151.6	35.20	132.0	0.267	22.000	139.0	1800
171.5	39.30	149.2	0.263	24.800	147.8	1910
203.1	47.30	177.0	0.263	29.400	160.8	2080

Table 5. (continued)

Grid VII

q (mm alcohol) density=0.804	ΔP (mm alcohol) density=0.804	q'=0.87q	ΔP/q'	q' (lb/ft^2)	V (ft/sec)	$R=\frac{\rho VW}{\mu}$
4.4	6.05	3.8	1.595	0.625	23.8	808
7.6	8.05	6.6	1.222	1.088	31.3	1060
19.6	18.10	17.1	1.058	2.820	50.5	1710
38.7	31.20	33.7	0.926	5.550	70.7	2400
59.3	45.20	51.5	0.878	8.480	87.5	2970
81.1	61.30	70.5	0.869	11.610	102.0	3460
103.0	77.40	89.7	0.864	14.790	115.5	3920
123.9	90.50	107.8	0.839	17.750	126.6	4300
141.4	102.60	123.0	0.831	20.250	135.0	4580
154.9	114.80	134.8	0.854	22.200	141.4	4800
168.0	120.80	146.2	0.826	24.100	147.4	5000
179.9	130.90	156.5	0.837	25.800	152.4	5180
189.0	136.90	164.5	0.833	27.100	156.4	5310

Table 5. (continued)

Grid VIII

q (mm alcohol) density=0.809	ΔP (mm alcohol) density=0.809	q'=0.87q	$\Delta P/q'$	q' (lb/ft^2)	V (ft/sec)	$R=\frac{\rho VW}{\mu}$
4.9	6.05	4.3	1.408	0.711	25.1	878
7.5	8.05	6.5	1.238	1.077	30.9	1080
20.9	15.10	18.2	0.832	3.100	52.4	1830
39.4	27.20	34.3	0.793	5.670	71.0	2480
60.4	41.30	52.5	0.786	8.700	87.8	3070
83.4	55.40	72.5	0.764	12.000	103.0	3600
106.7	71.40	92.6	0.772	15.320	116.4	4070
129.1	83.50	112.5	0.742	18.620	128.6	4500
146.0	95.60	127.0	0.755	21.000	136.5	4770
161.9	102.70	140.8	0.731	23.300	143.8	5030
172.0	107.80	149.6	0.722	24.750	148.2	5180
184.4	117.80	160.5	0.734	26.550	153.3	5360
194.6	123.90	169.0	0.732	28.000	157.5	5510

Table 5. (continued)

Grid IX

q (mm alcohol) density=0.804	ΔP (mm alcohol) density=0.804	q'=0.87q	$\Delta P/q'$	q' (lb/ft^2)	V (ft/sec)	$R=\frac{\rho VW}{\mu}$
4.7	5.05	4.10	1.232	0.675	24.6	837
7.4	7.05	6.45	1.093	1.061	30.9	1050
20.4	13.10	17.70	0.741	2.910	51.2	1740
39.2	23.20	34.10	0.682	5.610	71.0	2420
59.9	35.20	52.10	0.676	8.570	88.5	3000
84.4	46.30	73.40	0.632	12.090	104.5	3560
107.9	58.40	93.80	0.623	15.450	118.0	4010
126.8	69.40	110.30	0.628	18.150	128.0	4350
145.6	77.50	126.60	0.613	20.800	137.0	4660
162.0	86.50	141.00	0.613	23.200	144.8	4930
176.1	92.60	153.20	0.604	25.200	150.8	5130
187.4	96.60	163.10	0.592	26.850	155.8	5300
197.4	103.70	172.00	0.603	28.300	160.0	5440